

UCLA

UCLA Electronic Theses and Dissertations

Title

Dye analysis of archaeological Peruvian textiles using surface enhanced Raman spectroscopy (SERS)

Permalink

<https://escholarship.org/uc/item/5699m0tt>

Author

Burr, Elizabeth

Publication Date

2016

Peer reviewed|Thesis/dissertation

UNIVERSITY OF CALIFORNIA

Los Angeles

Dye analysis of archaeological Peruvian textiles using surface enhanced Raman
spectroscopy (SERS)

A thesis submitted in partial satisfaction of the requirements for the degree Master of
Arts in Conservation of Archaeological and Ethnographic Materials

by

Elizabeth Burr

2016

ABSTRACT OF THESIS

Dye analysis of archaeological Peruvian textiles using surface enhanced Raman spectroscopy (SERS)

by

Elizabeth Anne Burr

Master of Arts in Conservation of Archaeological and Ethnographic Materials

University of California, Los Angeles, 2016

Professor Ioanna Kakoulli, Chair

Surface-enhanced Raman spectroscopy (SERS) is an emerging technique for the identification of colorants at low concentrations, making it ideal for degraded and irreplaceable archaeological materials. Using silver nanoparticles (AgNPs) as the SERS platform, this research on the identification of textile dyes compares direct on-the-fiber extractionless analyses with micro-extraction methods employing hydrofluoric acid vapor, formic acid, and hydrochloric acid solutions. Seven red samples from Wari and Malena textiles from the site Huaca Malena in Peru and reference yarns dyed with *Relbunium* and cochineal were analyzed using individual fiber samples. Complementary analysis of archaeological samples was conducted with fiber optics reflectance spectroscopy (FORS). Carminic acid, the primary colorant of cochineal, and pseudopurpurin and purpurin, the main coloring compounds of *Relbunium* were detected in the reference samples. Three archeological samples provided potential matches for carminic acid and two may contain purpurin and pseudopurpurin. FORS, data indicate that all the archaeological samples contained cochineal.

The thesis of Elizabeth Anne Burr is approved.

Ioanna Kakoulli, Committee Chair

Charles S. Stanish

Dino DiCarlo

Elena Phipps

Diana Rambaldi

University of California, Los Angeles

2016

Acknowledgements

Thank you to my panel readers for their valuable comments and feedback. Thank you to the Conservation Science lab at LACMA (Diana Rambaldi, Terry Schaefer, Charlotte Eng, Laura Maccarelli, and Frank Pruesser) for allowing me to conduct research in their lab, and for all their generous teaching and assistance without which this project would not have been possible.

Thank you to Vanessa Muros for sure suggestion to pursue this project, for sharing archaeological samples from Huaca Malena, for advice and support on dye analysis, and assistance in Spanish translations. Thank you to Rommel Ángeles Falcón for providing samples and information from the Huaca Malena textiles, and tour the Huaca Malena archaeological site and museum. I am greatly appreciative of the assistance and advice provided by UCLA Material Science and Engineering PhD students Xiao Ma, Yuan Lin, and Roxanne Radpour. Their interest and technical support has been crucial to completing this thesis. Also thank you to Sergey Prikhodko for assistance and training on the SEM and Raman spectrometer. Thank you to Christian Fischer, Ioanna Kakoulli and Lesley Day for feedback and assistance on FORS. Thank you to my cohort for their support. Thank you to Getty for funding the UCLA/Getty conservation program.

Table of Contents

Chapter 1 Introduction.....	1
1.1 Background.....	1
1.2 Aims and scope of study.....	2
Chapter 2 Natural Dyes and Dyeing.....	4
2.1 Natural dyes.....	4
2.2 Mordants.....	5
2.3 Natural red dye sources of Peru	6
2.3.1. <i>Cochineal</i>	6
2.3.2. <i>Rubiaceae Relbunium</i>	7
2.3.3. <i>Rubiaceae Galium</i>	9
2.3.4. <i>Other red dyestuffs</i>	10
Chapter 3 Pre-Columbian Archaeological Evidence in Peru	11
3.1 Archaeological evidence and significance of textile traditions	11
3.2 Analysis of Pre-Columbian Peruvian Textiles	12
3.2.1. <i>Early Horizon</i>	13
3.2.2. <i>Early to Late Intermediate Periods (A.D. 200 to 1476)</i>	14
3.2.3. <i>The rise of cochineal red</i>	15
3.3 Archaeological Site of Huaca Malena	16
Chapter 4 Dye analysis & SERS.....	18
4.1 Dye Analysis	18
4.2 Surface Enhanced Raman Spectroscopy (SERS).....	18
4.3 SERS dye analysis	20
4.3.1. <i>SERS techniques and advances</i>	20
4.3.2. <i>Applications of SERS for the identification of cochineal and Relbunium</i>	22
Chapter 5 Materials and Methods	22
5.1 Sample materials.....	22
5.1.1. <i>Chemical standards and reference materials</i>	22
5.1.2. <i>Archaeological materials</i>	23

5.2 Microscopy and image analysis	24
5.2.1. <i>Optical microscopy of fiber samples</i>	24
5.2.2. <i>Scanning electron microscopy of fiber samples and AgNPs</i>	24
5.2.3. <i>Image analysis of fiber samples and AgNPs</i>	25
5.3 Fiber optic reflectance spectroscopy (FORS) of AgNPs and archaeological samples.....	25
5.4 Surface Enhanced Raman Spectroscopy (SERS).....	25
5.4.1. <i>Sample preparation</i>	25
5.4.2. <i>Synthesis of Silver nanoparticles (AgNPs)</i>	27
5.4.3. <i>SERS and Raman spectromicroscopy</i>	28
Chapter 6 Results and Discussion	29
6.1 Characterization of AgNPs.....	29
6.2 Characterization of archaeological textiles and fiber type.....	31
6.2.1. <i>Fiber and yarn type</i>	31
6.2.2. <i>Condition of archaeological fibers</i>	35
6.3 Characterization of reference dyes using SERS.....	37
6.3.1. <i>Extractionless on-the-fiber SERS</i>	38
6.3.2. <i>On-the-fiber SERS with HF micro-extraction</i>	40
6.3.3. <i>On-the-fiber SERS with formic acid micro-extraction</i>	42
6.3.4. <i>Liquid micro-extraction with HCl in MeOH and H₂O</i>	44
6.3.5. <i>Summary of findings from SERS methods</i>	48
6.4 Dye characterization of archaeological samples using SERS and FORS.....	50
6.4.1. <i>Extractionless on-the-fiber SERS</i>	50
6.4.2. <i>On-the-fiber SERS with formic acid micro-extraction</i>	51
6.4.3. <i>Liquid micro-extraction with HCl in MeOH and H₂O</i>	54
6.4.4. <i>FORS analysis of archaeological samples</i>	56
6.4.5. <i>Summary of findings</i>	57
Chapter 7 Conclusions.....	59
7.1 SERS performance.....	59
7.2 Future research	60

Table of figures and tables

Figures

Figure 1. TOP ROW (Images and information courtesy of Rommel Ángeles Falcón) A (sample VM01): camelid warp and weft bag, eccentric tapestry technique, mountain style; B(sample T-130A): cotton warp and camelid weft band, eccentric tapestry technique, Wari style; C (sample VM04): undyed cotton and dyed camelid polychrome band, double weave technique; D (sample 061.02.01): camelid, tapestry technique, Wari/Malena style. BOTTOM ROW (information courtesy of Rommel Ángeles Falcón): E (sample T-69): cotton warp camelid weft cloth, slotted tapestry technique, Malena style; F (sample 77.10.02):, cotton and camelid corner of cloth, brocade technique, Malena style; G (sample 119.000.029): camelid warp and weft uncu fragment, eccentric tapestry technique, Wari style.24

Figure 2. Secondary electron micrographs of AgNPs. Two different batches of AgNPs (right micrograph: Yuan Lin 2015) displaying round faceted particles along with rods (left image) and some wires (right image).30

Figure 3. Raman spectra of centrifuged batch 1 AgNPs analyzed within the first few days after synthesis (A) compared to the same expired batch analyzed three months later (B). Both spectra were acquired using a 785nm laser at 0.25% laser strength for 10 seconds and 1 acquisition after using KNO_3 to aggregate AgNPs. Raman spectra of centrifuged batch 2 AgNPs analyzed within the first few days after synthesis (C) compared to the same batch analyzed one month later (D). Both spectra were acquired using 633nm laser at 0.25% laser strength for 10 seconds and 1 after using KNO_3 to aggregate AgNPs. The large peaks at 1050 cm^{-1} are due to the KNO_3 added to the AgNPs.30

Figure 4. VM 01 photomicrographs: yarn samples images with digital microscope (A-B), cuticular scale pattern imaged with SEM (C), and interrupted medulla imaged with transmitted light (D).32

Figure 5. T-130A photomicrographs: yarn samples images with digital microscope (A-B), cuticular scale pattern imaged with SEM (C), and interrupted medulla imaged with transmitted light (D).33

Figure 6. VM 04 photomicrographs: yarn samples images with digital microscope (A-B), cuticular scale pattern imaged with SEM (C), and interrupted medulla imaged with transmitted light (D).33

Figure 7. 061.02.01 photomicrographs: yarn samples images with digital microscope (A-B), cuticular scale pattern imaged with SEM (C), and interrupted medulla imaged with transmitted light (D).33

Figure 8. T-69 photomicrographs: yarn samples images with digital microscope (A-B) and uninterrupted medulla imaged with transmitted light (C).34

Figure 9. 77.10.02 photomicrographs: yarn samples images with digital microscope (A-B) and interrupted medulla imaged with transmitted light (C).34

Figure 10. 119.000.02 images: digital microscope (top) and transmitted light image of interrupted medulla (bottom).35

Figure 11. Secondary electron micrographs of archaeological samples covered in burial contaminants both before rinsing in ethanol (A-B) and after rinsing (C-D) of VM03 (A), T-130A (B), VM01 (C) and VM04 (D).36

Figure 12. SEM images of VM01 (A) T-130A (B) and VM04 (C) showing cracking and breaking in the brittle fibers.37

Figure 13. Secondary electron micrographs of fibers from sample T-130A, displaying crease and folds in the fiber, perhaps do to exposure to an alkaline environment during burial.37

Figure 14. Transmitted light images of T-69 and 77.10.02 displaying distortion and splitting....37

Figure 15. Raman spectra of on-the-fiber analysis without extraction on unmordanted (A) and mordanted (C) cochineal reference fiber, and 0.001M carminic acid in ethanol (B). Spectra were acquired using 785nm laser at 0.25% for 10 seconds at UCLA. Unmordanted cochineal spectrum (A) courtesy of Diana Rambaldi, acquired at LACMA using 785nm laser at 1% for 5 sec with 3 accumulations.39

Figure 16. Raman spectra of on-the-fiber analysis without extraction of unmordanted *Relbunium hypocarpium* reference fibers (A and B) compared to purpurin (C) and pseudopurpurin (D). *Relbunium* samples (A and B spectra) acquired using 785nm laser at 0.05% for 10 sec at UCLA. Purpurin (C) acquired using 785nm laser at 0.25% for 10 sec at UCLA. Pseudopurpurin (D) was acquired at LACMA using 785nm laser at 1% for 5 sec.40

Figure 17. Raman spectra of HF micro-chamber extraction of unmordanted cochineal reference fibers (A and B) compared to 0.001M carminic acid combined with 5%HCl (C). Cochineal samples (A and B) acquired at LACMA using 785nm laser at 1% for 5 sec with 5 co-adds. Carminic acid (C) acquired using 785 nm laser at 0.25% for 10 sec at UCLA.41

Figure 18. Raman spectra of HF micro-chamber extraction of *Relbunium* reference fibers mordanted *R. ciliatum* (A) and unmordanted *R. hypocarpium* (B) compared to pseudopurpurin (C) reference fiber extracted using the same technique. All spectra obtained using 785nm laser at LAMCA, A and C: 1% for 5 sec, B: 1% for 5 sec with 5 co-adds.....42

Figure 19. Raman spectra of 25% formic acid extraction from mordanted cochineal reference fibers acquired both off the fiber (A) and on the fiber (B) compared to 0.001 M carminic acid (C). All spectra obtained at UCLA using 785nm laser at 0.25% for 10 sec.43

Figure 20. Raman spectra of 25% formic acid on-the-fiber extraction from mordanted *R. ciliatum* (A) compared to pseudopurpurin chemical standard (B). A at UCLA using 785 nm laser at 0.25% for 10 sec with 2 accumulations. B acquired at LACMA using 785nm laser at 1% for 5 sec.....44

Figure 21. Raman spectra of liquid extraction using HCl in MeOH and H₂O on mordanted cochineal reference fibers (A and B) compared to 0.001M carminic acid combined with HCl in MeOH and H₂O both unheated (C) and heated for 10 minutes (D). The large peak at 1050 cm⁻¹ in the spectrum B is due to the KNO₃ added to the AgNPs. Spectra acquired at UCLA with the following parameters: A: 785nm laser at 0.25% for 10 seconds; B: 633nm laser at 0.25% for 10 seconds, C: 633nm laser at 0.01% for 10 seconds; D: 633nm at 0.25% for 10 seconds with 2 accumulations.....45

Figure 22. Raman spectra of 0.001M purpurin combined with HCl in MeOH and H₂O both unheated (A) and heated for ten minutes (B) compared to 0.001M solutions of purpurin (C) and alizarin (D). Spectra acquired at UCLA with the following parameters: A: 633nm laser at 0.01% for 10 seconds with 2 accumulations; B: 633nm laser at 0.25% for 10 seconds; C: 633nm laser at 0.25% for 10 seconds with 2 accumulations; D: 785nm laser at 0.25% for 10 seconds with 2 accumulations.....47

Figure 23. Raman spectra of liquid extraction using HCl in MeOH and H₂O on mordanted *Relbunium ciliatum* reference fibers (A and B) compared to 0.001M solutions of purpurin combined with HCl in MeOH and H₂O both unheated (C) and heated (D). *Relbunium* provided very inconsistent spectra and unclear match to any chemical standard. Spectra acquired at UCLA with the following parameters (listed by spectrum color): Black: 785nm laser at 0.25% for 10 seconds; Blue: 633nm laser at 0.25% for 10 seconds; Green: 633nm laser at 0.1% for 10 seconds with 2 accumulations; Red: 633nm laser at 0.25% for 10 seconds.....48

Figure 24. Raman spectra of sample T-130A based on extractionless on-the-fiber SERS without extraction (A and B) compared to carminic acid (C) and purpurin (D) both at neutral pH. The peaks at 1050 cm^{-1} in spectra A & B are due to the KNO_3 in the AgNPs. All data acquired using 785 nm laser.51

Figure 25. Raman spectra of sample T-69 analyzed using 25% formic acid (A) compared to *Relbunium ciliatum* analyzed with the same method (B) and pseudopurpurin standard (C). Neither spectrum was reproducible, though both (A and B) share common peaks with pseudopurpurin. The large peak at 1050 cm^{-1} in spectrum A is due to the KNO_3 added to the AgNPs. Spectra A and B were acquired at UCLA using 785 nm laser at 0.25% for 10 sec, B with 2 accumulations. Spectrum C was acquired at LACMA using 785nm laser at 1% for 5 sec.51

Figure 26. Raman spectra of sample 119.000.029 prepared with 25% formic acid (A) compared to *Relbunium* with the same preparation (B) and pseudopurpurin chemical standard (C). Spectra A and B were acquired at UCLA using 785 nm laser at 0.25% for 10 sec with 2 accumulations. Spectrum C acquired at LACMA using 785nm laser at 1% for 5 sec.53

Figure 27. Raman spectra of sample 119.000.029 prepared with 25% formic acid (A) compared to carminic acid at neutral pH (B). Spectra acquired at UCLA using 785nm laser at 0.25% for 10 seconds, A with two accumulations. The large peak at 1050 cm^{-1} in spectrum A is due to the KNO_3 added to the AgNPs.54

Figure 28. Raman spectra of archaeological sample 77.10.02 (A and B) and sample 119.000.029 (C and D) extracted with heated HCl compared to carminic acid prepared with HCl without heating (E) and with heating (F). All spectra acquired at UCLA using 633nm laser at 0.25% for 10 seconds and 2 accumulations with the following exceptions: D acquired at 0.01% strength; A and B acquired with 1 accumulation. The large peaks at 1050 cm^{-1} are due to KNO_3 in the AgNPs.55

Figure 29. Archaeological samples VM04 (A) and 61.02.01 (B) extracted with heated HCl compared to carminic acid prepared with HCl without heating (C) and with heating (D). All samples acquired at UCLA using 633nm laser at 0.25% for 10 seconds with 2 accumulations. The large peaks at 1050 cm^{-1} are due to KNO_3 in the AgNPs.56

Figure 30. FORS reflectance data of archaeological samples indicating absorption maxima characteristic of cochineal red.....57

Tables

Table 1. Anthraquinone dye molecules identified in red dyes. Carminic acid is the predominate compound in cochineal dye. The other compounds listed are found in plant based red dyes to varying proportions depending on the source. The primary constituents of *Relbunium* derived dye are pseudopurpurin and purpurin, with smaller quantities of munjistin. Alirarin, which is common in cultivated old-world madder is absent from *Relbunium*. 9

Table 2. Full Width at Half Height measurements of two batches of silver nanoparticles used in this study.....29

Table 3. Ply/spin notation follows method used in other studies on textiles from Huaca Malena, where the first letter designates the ply direction, and the number and letter in parenthesis designates the number of threads and their spin direction. Fiber diameter measurements, taken from 15 data points were acquired from photomicrograph of a yarn and measured in ImageJ. .32

Chapter 1 Introduction

1.1 Background

The masterful textile traditions of Peru have a long history, which continue today. The development of these traditions is documented in the archaeological record, primarily through preserved mummy bundles recovered from sites on the extremely dry coastal desert of Peru. Many of the textiles are finely woven and brilliantly colored, often with organic dyes.¹ Through site-based study of textile traditions, an understanding of regional textile traditions can be reconstructed. The dyestuff used can provide information and help map not only the development of dyeing technology within different societies, but also the selection and procurement of natural resources, regional and interregional exchange and economics as well as craft specialization and movement of people. To identify the source of the dyestuff, it is imperative to conduct a thorough analysis of the dye at the molecular scale; as Max Saltzman, researcher on Peruvian dyes said: “you can’t tell a dye by its color” [1]. The identification of dyes present in a textile is inherently challenging given the nature of dyes, which 1) are very effective colorants despite being present in very small quantities, 2) are chemically bonded to fibers and usually require separation for chemical identification, and 3) degrade over time. Once a chemical signature is identified from a textile sample, further research is required to determine the source of the dye, which requires a reference library of analyzed dyes for comparison and identification. In the last decade, surface-enhanced Raman spectroscopy (SERS) has been applied for the characterization of dyes in art and archaeology, and new techniques and methodologies have been developed to improve detection. While there are a number of successful techniques available for dye analysis, the primary benefit of SERS is the minute sample size needed (<500 μm), which represents a small fraction of an individual fiber strand and a much less quantity compared to segments of yarn pieces required for other techniques.

¹ Archaeological Peruvian textiles also include inorganic colorants, however this study is concerned exclusively with organic dyes. Inorganic colorants and their analysis are not included.

1.2 Aims and scope of study

The aim of this study is two-fold: to investigate different SERS methodologies optimized for the analysis of archaeological colored textiles, and characterize the red dyes used to color the textiles found at the pre-Columbian archaeological site of Huaca Malena in Peru. The Saltzman reference collection [2-4]² and chemical standards provide reference materials of red dyes (and their coloring compounds) used in ancient Peru; specifically cochineal (a dye extracted from the *Dactylopius* scale insect) and *Relbunium* (a dye produced from the roots of brush plants in the genus *Relbunium*). This research tests methods for extractionless and on-the-fiber micro-extraction of the dye molecules to compare SERS spectra from chemical standards of carminic acid (the primary coloring compound of cochineal) and purpurin and pseudopurpurin (the primary coloring compounds in *Relbunium*) to those from reference yarns in the Saltzman collection dyed with cochineal and *Relbunium*.

These known references were compared to red dyes from seven textiles recovered from different burials at Huaca Malena on the coast of Peru for the purpose of dye identification. The research compares the following extractionless and extraction techniques for dye analysis and characterization employing SERS:

1. On-the-fiber extractionless analysis
2. Micro-extraction with hydrofluoric acid (HF) vapor with analysis on-the-fiber
3. Micro-extraction with formic acid in ethanol (EtOH) with analysis on-the-fiber
4. Liquid micro-extraction using hydrochloric acid (HCl) with water and methanol (MeOH)

Chapters 2-4 provide literature review and background information on pertinent subjects and information on dyes and specifically those from Peru (Chapter 2); a summary of dye analysis

² This reference library of traditional Peruvian dyes was created by chemist and dye expert Max Saltzman in 1977 from plant and animal sources collected in Peru. This collection has been used as reference samples for a number of studies on Peruvian dyes, including the studies cited here.

from Peruvian archaeological textiles (Chapter 3); an overview of Huaca Malena (Chapter 3), and overview of SERS (Chapter 4). Chapters 5-7 contain the experimental sections of this study, split into materials and methods (Chapter 5), results and discussion (Chapter 6), and conclusion (Chapter 7).

Chapter 2 Natural Dyes and Dyeing

2.1 Natural dyes

Natural dyes, which originate from plant and animal sources, are composed of organic molecules that have visible color properties produced by their chromophores (conjugated pi-bond systems) and auxochrome functional groups (ex. hydroxyl groups, carboxyl groups, amino groups, and sulphonic acid groups) [5, 6]. These molecules are also highly fluorescent.

Electrons in the pi-bond systems absorb photons of particular energies defining their color in the visible electromagnetic range and become excited, then transfer to a higher energy level before reemitting the absorbed energy at a higher wavelength due to loss of energy during molecular relaxation (internal non-radiative energy transitions). Colorfast dyes appropriate for textile dyeing also form bonds with the fibers. To transfer the colorant to the fibers being dyed, the dye molecules are first extracted from the dyestuff into water to create a dyebath. Dyeing can occur through a number of chemical reactions based on the chemical properties of the dyestuff and fiber. The most common dye types based on their properties are direct [5-7]³, vat [7, 8]⁴, anionic or cationic dyes [6]⁵, and mordant dyes.

The dyes included in this study, *Relbunium* and cochineal, are both classified as mordant dyes.

Mordant dyes require a polyvalent metal ion to hold fast the dye molecule to the fiber. Most dyestuffs require mordanting, though any dye can be affixed using this technique. During this

³ Direct dyes are composed of water-soluble compounds which have an affinity for the substrate and bond readily through a number of chemical bond types. This technique is especially appropriate for cellulosic fibers, which swell and absorb the dye compounds when introduced to the hot dye bath. There are few dyestuffs that qualify as direct dyes and they generally have poor color fastness. Some direct dyes include safflower and orchil containing lichen which can be used to dye proteinaceous fibers.

⁴ Vat dyes are insoluble in water and must undergo chemical reduction under widely varied and often complex processes. Vat dyes achieve affinity for both cellulosic and proteinaceous fibers in the bath, after which the dye is oxidized in air to achieve its color on the fiber substrate. There are few vat dyestuffs though these are among the most significant in history. These include species of indigo found throughout the world and shellfish purple, including *Concholepas concholepas* in Peru, *Plicopurpura pansa* in Mexico and *Murex brandaris* (known as Tyrian purple) in the Mediterranean.

⁵ These dyes ionize in water, and form ionic bonds to fibers. This type of dyeing is far more common in synthetic dyes though one natural dye that falls into this category is berberine.

process, the dye forms complexes (organometallic compounds) with the metal salt used as the mordant, which then attaches firmly to the fiber. Mordant dyes bond readily to proteinaceous animal fibers, however cellulosic plant fibers can be more difficult to dye with this technique and require pretreatment. In addition to fiber type, mordant, and dye, the pH and temperature are important variables to the success of a mordant bath.

2.2 Mordants

A variety of substances including metal salts are used as mordants all of which contribute properties to the final color and light fastness. Among the most common mordants are the potash alum chemical compound (hydrated potassium, aluminum sulfate $KAl(SO_4)_2 \cdot 12H_2O$), salts of iron (Fe), tin (Sn), and copper (Cu). Plants with a high mineral content are also used as mordants and when no natural sources are available, mordants have also been manufactured in some regions of the world [7]. Potash alum found in abundance in deserts and volcanic regions has been commonly used as a mordant throughout the world for animal and plant fibers, typically yielding bright colors. Plants which absorb large quantities of aluminum provide an altered color compared to a potash alum mordant [7].

Iron is a common mordant more compatible with plant fibers than animal as it is known to degrade proteinaceous fiber. Iron provides dull colors compared to alum and is often used in combination with plant tannins to yield brown and black colors [7]. There are many different sources for iron mordants, the most common of which includes rusted iron objects or iron rich muds or clay. In the mountains and deserts of Peru, iron and alum are often found together, where they are referred to in Quechua language as *colpa* or *alcaparosa* [2]. In the highlands of Peru, copper rich clay is also used as a mordant, which provides a green color to wool without a dye present.⁶

⁶ Unpublished correspondence with Jenny Figari at Yachay Wasi

2.3 Natural red dye sources of Peru

Contemporary dyers and weavers in Peru hold knowledge on dyestuffs and dyeing traditions, and are a primary source of information on the study of Peruvian dyes. Studies on contemporary and traditional uses of dyes includes works by Ana Roquero [8] on dyestuffs from the Americas, studies summarized by Antunez de Mayolo [2], and research underway by Yachay Wasi in Lima, Peru [9] and the British Museum [10]. There are also a number of prominent authors on the chemistry and history of dyeing such as Helmut Schweppe [11, 12], Judith Hofenk de Graaf [5], and Dominique Cardon [7] and current chemical research on Peruvian dyes including work by Nathalie Boucheri [13] and the Rambali et al publication in 2015 [14]. The discussion on natural red dyes available from Peru draw on these studies on contemporary, historical, and chemical aspects of these dyes. The two primary natural sources for red dye locally available within Peru are cochineal derived from insects (*Dactylopius coccus*), and *Relbunium sp.* derived from scrub bush. Other less common sources of red dyes include the plant sources *Gallium*, *Bixa*, and *Caesalpinia*.

2.3.1. Cochineal

Cochineal, *magno* or *macnu* in Quechua, derives from female *Dactylopius* scale insects found on nopal cacti of the genera *Opuntia* and *Nopelea* [7, 8]. The dye is extracted from the insect body in a hot dye bath, and requires a mordant to fix to the fibers. Cochineal is known for its deep crimson red though the color can be altered by additives, changes in the pH, the type of mordant utilized and the water quality resulting to hues ranging from orange to purple [7, 15]. Tin mordant in particular creates scarlet color while an iron mordant can provide a purple hue. Weathering and natural aging of textiles dyed with cochineal also affects the color. Pure cochineal has been identified from a number of archaeological samples including browns and yellows, many of which may be altered from the original color [7, 16].

Cochineal is composed primarily of the anthraquinone carminic acid (94-98%) with traces of kermesic acid, flavokermesic acid and an unknown component called dcII, the quantity of which is known to vary by species [5, 16]. The term “cochineal” is used to refer to dyes derived from all species of *Dactylopius*, though a distinction is made between wild and cultivated cochineal. The cultivated species *Dactylopius coccus* is found in both western Mexico and Peru, though the prehistoric distribution of this species is not fully understood. The cultivation of *D. coccus* was perfected in western Mexico, though the extent of cultivation in Peru is not known and may have been collected rather than farmed [7]. *D. coccus* appears to be indigenous to Peru based on DNA analysis, and may have been introduced to Mexican regions via established sea trade routes in pre-Columbian times [17]. Wild species indigenous to Peru include *D. confuses*, *D. ceylonicus* and *D. tomentosus*, though their quality as a dyestuff is poor relative to *D. coccus* [18]. It has also been suggested that *D. confuses* was the source of cochineal red in pre-Columbian Peru, rather than *D. coccus* [16]. When the Spanish arrived in Peru however, cultivated cochineal (*D. coccus*) was found in abundance both on the south coast and the south central highlands regions [19]. Cultivated cochineal is best known as valued global trade good. Between the sixteenth and eighteenth centuries, cochineal was exported from the Americas by the ton and traded throughout the world, largely replacing other Old World insect reds such as kermes and Armenian cochineal [19, 20].

2.3.2. Rubiaceae *Relbunium*

Relbunium, known as chapi-chapi, chchapi, or antaco in Quechua, is a dye plant indigenous to Central and South America [7, 21]. *Relbunium* dye is derived from the roots of the plant, which are soaked prior to dyeing. A alum mordant and weak acid solution provide a red color, while a more acidic dye bath creates an orange dye [18]. While plant reds including *Relbunium* are known to provide a more orangey red, the water source, mordant, and additives can create a brilliant red or purple hue with this dye.

The genus *Relbunium* belongs to the subfamily Rubiaceae (Rubioideae) as is the better known Old World dyestuff known as madder, including the species *Rubia tinctorum* (cultivated species) and *Rubia peregrina* (wild madder) [5, 22]. There are twenty-five known species of *Relbunium* found throughout the Americas, seven of which are found within Peru: *R. ciliatum* (used in this study), *R. microphyllum*, *R. nitidum*, *R. gibemium*, *R. tetragonum*, *R. hirsutum*, and *R. richardianum* [3]. *R. hypocarpium* (used in this study) is indigenous to northern Chile. The habitat range of *Relbunium* varies by each species, but it is generally found at higher altitudes in non-arid regions. *R. hypocarpium* is found in high altitude tropical regions of the Americas on hillsides and open areas of humid brush or forest habitats at altitudes between 1,000 and 3,000 meters [8]. *R. nitidum* however is native to the lomas regions (coastal deserts) in Peru and Chile [23]. While the coast is low altitude and extremely dry, the lomas regions are in the foothills of the river valleys that cut through the landscape.

Relbunium and madder dyes are comprised of anthraquinone molecules (Table 1). Similar to the wild madder species *Rubia peregrina*, *Relbunium* dye is composed primarily of pseudopurpurin, purpurin and smaller quantities of munjistin, and other anthraquinones [5]. Unlike the cultivated madder species *Rubia tinctorum*, alizarin is absent from both *Relbunium* and *Rubia peregrina* [5]. Under certain conditions including an acidic environment, pseudopurpurin loses its carboxyl group producing purpurin and carbon dioxide. This decomposition may occur in the dyestuff to varying degrees during drying, aging, and dyeing processes, and during sample preparation involving wet chemistry [24, 25]. As a result, *Relbunium* dye is characterized by the presence of either purpurin or pseudopurpurin and the absence of alizarin [5]. Dyes derived from different species of *Relbunium* are difficult to distinguish, though subtle differences occur in the content of glycosidic precursors of anthraquinones [7]. The primary distinction between *R. ciliatum* and *R. hypocarpium* (both used

in this study) is the high proportion of lucidin-3-O- β -primeveroside in the former, however once absorbed to a fiber, the two species of dyestuff appear to be chemically indistinguishable [7].

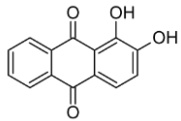
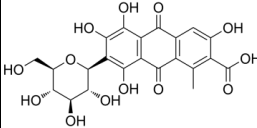
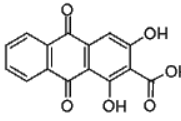
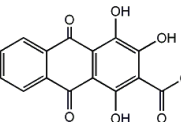
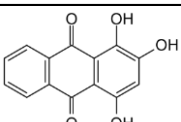
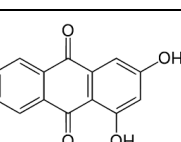
ANTHRAQUINONES		
common name	IUPAC nomenclature	chemical structure
alizarin	1,2-dihydroxyanthraquinone	
carminic acid	3,5,6,8-tetrahydroxy-1-methyl-9,10-dioxoanthracenecarboxylic acid	
munjistin	1,3-dihydroxy-2-anthraquinonecarboxylic Acid	
pseudopurpurin	1,2,4-trihydroxy-3-anthraquinonecarboxylic Acid	
purpurin	1,2,4-trihydroxyanthraquinone	
xanthopurpurin	1,3-Dihydroxyanthraquinone	

Table 1. Anthraquinone dye molecules identified in red dyes. Carminic acid is the predominate compound in cochineal dye. The other compounds listed are found in plant based red dyes to varying proportions depending on the source. The primary constituents of *Relbunium* derived dye are pseudopurpurin and purpurin, with smaller quantities of munjistin. Alirarin, which is common in cultivated old-world madder is absent from *Relbunium*.

2.3.3. Rubiaceae Galium

Galium is a red dyestuff in the same subfamily as *Relbunium* and madder (*Rubiaceae*) [5, 22], and is referred to in Quechua as *ccallo-huacta* or *galio*, but is also referred to as *antaco* or *chapi-chapi*, which are the Quechua names for *Relbunium* [16]. *Galium* is a mordant dye derived from the roots of the plant similar to *Relbunium* [8].

The phylogeny of the *Galium* and *Relbunium* genera has been re-categorized many times and some species of *Relbunium* were once classified as *Galium*. Species of *Galium* are found throughout the world in damp areas such as swamps and stream banks, and a number of species are found in Peru. Old World species are chemically indistinguishable from cultivated madder species, identified by the anthraquinones alizarin, purpurin, pseudopurpurin, rubiadin, and xanthopurpurin [5, 26]. Despite the similarities between the two, species of *Galium* can be distinguished from *Relbunium* by the presence of alizarin, which is absent from *Relbunium* [16].

2.3.4. Other red dyestuffs

Bixa orellana is a scrub which is used as a direct dye producing a yellow to red colorant and known by many names, the most common being *achiote* and *annatto* in Spanish, and in Peru as *guandur*, *huantura*, *mandur*, and *urucu*. It is found in both wet and dry climates below 1,000 meters in tropical and subtropical regions of the Americas [7, 8]. This source is sometimes mentioned as a red dye, but appears to be far more commonly utilized for a yellow or orange color. *Bixa* is comprised primarily of the apocarotenoid bixin, the secondary compounds of which produce red [5]. Bixin is soluble in fats, though must be treated with an alkali to be soluble in water. The seeds are ground into a powder and mixed with animal fat and water to color plant fibers such as palm [27]. It was historically used in Europe as an after treatment of cochineal dye to brighten the color [5].

Caesalpinia, known commonly as brazilwood, are hardwood trees whose heartwood is a source of red flavonoid dye. Though known as a fiery red dye, it is known to fade to a yellow-brown hue [5]. Species of *Caesalpinia* are found throughout Central and South America and were once common on the coast of Brazil, for which the country was named. *C.paipai* and *C. spinosa* are found in Peru, and their seed pods are used to create a grey or black dye, however the most ubiquitous species used as a red dye are not found in Peru [27].

Chapter 3 Pre-Columbian Archaeological Evidence in Peru

3.1 Archaeological evidence and significance of textile traditions

Though preservation of textiles in most climates is rare, the dry and stable burial conditions of coastal Peru provide an abundance of archaeological textiles and an opportunity to investigate an important but understudied ancient industry. There are tens of thousands of recovered archaeological textiles from Peru, many of which are elaborately dyed. Most examples originate from mummy bundles, which are comprised of individuals often positioned in a flexed position and wrapped in layers of textiles. These mummy bundles are found throughout the coast, in single or mass burials.

Textile manufacture in Peru is a tradition thousands of years old. The earliest textile evidence are plant-based cordage, twining, and weaving, such as fragments from Guitarrero Cave in north-central highlands of Peru, firmly dated between 8,000 to 10,000 B.C. using accelerator mass spectrometry radiocarbon dating [28]. While plant materials such as cotton are sometimes dyed, dyes became more common with the advent of textiles manufactured from camelid fibers versus plant. Archaeological and zooarchaeological evidence from Peruvian Andes signifies domestication of alpaca in the region occurred as early as 4000 B.C. [29]. While wool could be obtained from wild camelid species, the white fiber required for a clear and bright dye is associated with domesticated species bred for their fiber.

The Paracas culture in the Early Horizon period (900 to 200 B.C.) is known for their fine textile traditions covered with embroidered dyed camelid fibers depicting intricate anthropomorphic and zoomorphic iconography. Wari and Tiwanaku, two Middle Horizon states based in the highlands, are known for their very fine textiles with abstracted geometric motifs. These are typically tapestry woven textiles using a wide range of dyed yarns to create their motifs.

Undoubtedly, the production of these textiles was consuming of both time and resources. It is apparent that these objects were of cultural and economic value to the societies that made and used them, and both their raw materials and the textiles themselves were potentially important trade items. A better understanding of the raw materials used in textile production and the methods how these were processed and used can provide useful and important information on social and economic organization, traditions, and customs of ancient cultures in Peru.

3.2 Analysis of Pre-Columbian Peruvian Textiles

A number of researchers have analyzed Peruvian dye samples with a variety of techniques both for the purpose of testing new methodologies and as comprehensive studies on textile collections. According to archaeologist Ran Boytner [23], 283 samples were analyzed between 1934 and 1992 by a number of researchers. Many of these samples were the work of a prolific chemist Max Saltzman from the University of California Los Angeles (UCLA), who published extensively on the subject between 1963 and 1992. His analysis was based primarily on ultraviolet-visible transmission spectroscopy for the characterization of dyes from museum collections. Saltzman was also the creator of the reference collection used in this study as well as others [1, 4, 30, 31]. 157 of the samples are published in Wouters and Rosario-Chirinos 1992 publication. These researchers have used high-performance liquid chromatography with diode array detection (HPLC-DAD) to analyze samples from 42 textiles also sourced from museum collections [16]. In 2007, Zhang et al. [32] employed high-performance liquid chromatography, mass spectrometry (HPLC-DAD-MS) for the identification of yellow dyes. More recent analyses include museum collection based-studies using SERS by Leona et al. and Rambaldi et al. [14] as well as a large comprehensive study on textiles from northern Chile by Hans Barnard and Ran Boytner [33].

Between 1992 and 2001, the Andean Dye Research Project established between the UCLA and the Getty Conservation Institute (GCI) analyzed thousands of samples using ultraviolet-visible

transmission spectroscopy of extracted dye samples [23]. Their samples originated from three sites: two south coast sites in the Osmore River Valley, Chiribaya Alta and El Algodonal in Peru dating to later Middle Horizon to Late Intermediate Period (A.D. 950 to 1375) [3, 34] and the Late Intermediate Period Lambayeque site of Pacatnamu on the north coast (A.D. 1100 to 1370) [23]. These studies are significant because their samples are site based and provide a broader understanding to the implications for the uses of dyes within a society. Recently, another site-based study was published of dye analysis on textiles from San Pedro de Atacama in northern Chile including both local and Tiwanaku textiles dating to the Middle Horizon (A.D. 500-950) [35]. Based on the findings from dye analysis studies from the last few decades, there are trends over time and regions in the use of red dyes cochineal and *Relbunium* as discussed below.

3.2.1. Early Horizon

Relbunium was the predominant red dye in Early Horizon coastal periods (700 B.C. to A.D. 200), with much of this evidence deriving from the Paracas culture on the south coast [4, 16]. In a small number of instances, other red dyes have been identified from the Early Horizon period. Cochineal was detected from three Paracas textiles all from an individual mummy bundle (out of 141 Paracas samples studied from 40 bundles) [30]. Four samples from three Paracas textiles (out of 42 textiles sampled) found xanthopurpurin as the predominant dye molecule [16]. Xanthopurpurin is a reduced anthraquinone molecule, and likely derived from a species of *Rubiaceae*. While xanthopurpurin is found in *Galium*, it could be a component or degradation product derived from *Relbunium*.

Few textiles have been recovered from the highlands due to lack of preservation though there is evidence of access to red plant dyestuffs during the Early Horizon. A study on agriculture use near the lake Titicaca Basin noted the presence of both *Galium* and *Relbunium* as “weeds” with a dramatic increase in the occurrence of *Relbunium* between 250 B.C. to A.D. 500 [36]. Though

the study does not mention the use of either plant for dyeing, this evidence confirms local access to these dyestuffs, which were likely to be exploited.

3.2.2. Early to Late Intermediate Periods (A.D. 200 to 1476)

In a study of Peruvian textiles in the Metropolitan Museum of Art collection (MMA), the earliest consistent evidence of cochineal is derived from textiles associated with the Recuay culture from the northern central Andes between the highlands and the coast (A.D. 300-600) [37], and the Nazca culture (100 B.C. to A.D. 800) of the Early Intermediate period of the southern coast [19]. After these periods, the use of cochineal red appears to have flourished. High performance liquid chromatography (HPLC) analyses of 42 textiles attributed to the Paracas, Nazca, Wari, Tiwanaku, Chancay, Chimu, and Inca cultures from museum collections including the Royal Museum of Art and History in Brussels, Belgium and the Museo Nacional de Arqueología Antropología Lima, Peru revealed the earliest evidence of cochineal in the dataset associated with the Wari culture (A.D. 700-1100) [16]. In this study, all occurrences of plant derived red dyes associated with the Wari and Tiwanaku cultures were found in tandem with other dyestuffs (including cochineal) providing a wide range of colors. Textiles associated with the later Chancay, Chimu and Inca cultures provided no evidence of use of *Relbunium*.

Site-comprehensive data provide insight into the regional transitions from red plant dyestuffs to cochineal. In northern Chile in the San Pedro de Atacama landscape of the Middle Horizon (A.D. 500-900), all textiles of both regional and Tiwanaku styles were dyed with *Relbunium* [35]. Interestingly, according to this study the raw dyes and fibers used were imported, evidencing trade with the highland Tiwanaku [35]. In contrast, Tiwanaku style textiles found in museum collections contain both *Relbunium* and cochineal dyes [16]. The replacement of *Relbunium* by cochineal during the Middle Horizon of the Osmore River Valley in southern Peru coincides with the transition from one group (the Tumilaca) to another (the Chiribaya), a process potentially associated with the disbanding of the Tiwanaku culture in the highlands [34]. Textiles associated

with the Tumilaca, which are of much coarser weaving, were dyed with *Relbunium*, while Chiribaya textiles in the same region were more finely woven and exclusively dyed with cochineal [3].

Cochineal was identified in textiles of all social groups, whereas *Relbunium* was the most prevalent red found in non-elite sites at the northern coast Late Intermediate (A.D. 1100-1370) site of Pacatnamu of the Lambayeque culture [23]. This study identified *Relbunium* dyed cotton textiles while the elite red textiles dyed with cochineal were made of camelid fibers. Based on minimal evidence of camelid yarn production at this site and others suggests that pre-dyed camelid yarns were imported from the highlands to the coast [38]; implying cochineal was not a local resource. As mentioned above, during the same period, textiles associated with the Chancay (A.D. 1100-1470) suggest that *Relbunium* had fully replaced by cochineal by this period [16]. However, because these data on Chancay textiles are acquired from museum collections, they likely reflect primarily elite burials, as more valued textiles are likely to be acquired by major museums. The investigation of *Relbunium* in later periods of Peruvian archaeology would benefit from additional site-based analysis.

3.2.3. The rise of cochineal red

After the Early Horizon (900 B.C. to A.D. 200), cochineal was used with more regularity though the cause of the shift is unknown. There is speculation that cochineal was not widely used in Peru until it was imported from Mexico during the Early Intermediate Period (A.D. 200 to 600) [39]. Perhaps infrequent earlier uses of cochineal of the Paracas were derived from local wild varieties prior to the cultivation of cochineal. According to Phipps [19] cochineal became available perhaps due to an arid climate shift [40] in this region during the Middle Horizon Period. The presence of *Opuntia* cacti in pre-Columbian coastal Peru presumed that it was used for raising cochineal as a dyestuff, is confirmed by the presence of cacti needles in the material culture, and iconographic representations of cacti [41]. Coastal camelid textiles

associated with the highland cultures of Wari and Tiwanaku are mainly dyed with cochineal (rather than other red plant dyestuffs) strengthening the hypothesis that cochineal was most likely a highland resource introduced to the coast through interregional trade and cultural interactions. In the cases where cochineal and *Relbunium* are both present in textiles within an individual site, there is potential for interpretation on cultural affiliation, social status, and/or trade patterns. With more comprehensive site-specific dye analysis research, a greater understanding of textile traditions and their implications can be drawn.

3.3 Archaeological Site of Huaca Malena

The site of Huaca Malena located on the south Peruvian coast in the Asia Valley was first excavated in 1925 by Julio C. Tello and Toribio Mejia Xesspe, and later (in 1997) by Denise Pozzi-Escot and Rommel Ángeles Falcón [42]. In between the excavation seasons the site was heavily looted; however undisturbed burials were also recovered in the 1997 excavation season, which are housed at the Museo Municipal Huaca Malena near the excavation site. The site consists of a platform constructed of adobe with six smaller upper platforms containing ceramic and architectural styles that relate to Early Intermediate Period styles found in adjacent valleys to the north and south of the Asia Valley. After a period of abandonment at the beginning of the Middle Horizon (A.D. 600 to 1100), the structure was reused as a cemetery and intrusive tombs were dug into the platform. These tombs display four distinct types⁷ and consist of multiple mummy bundles within each tomb together with burial offerings. In total 350 bundles were excavated; 300 during the 1925 excavations by Tello, and another 50 in 1997 by Pozzi-Escot and Ángeles Falcón.

The majority of the 4000 textiles found on site are cotton, most of which are undyed, though some cotton textiles were dyed blue and orange [43]. Textiles with camelid are most often dyed and constructed with intricate motifs. Weaving tools were found exclusively in female burials at

⁷ corresponding to epochs 2b and 3 of the Middle Horizon

the site suggesting that textile manufacture in this region was a gender-specific craft. The textiles contain numerous stylistic attributions in addition to the local Malena styles [44]. A number of non-regional textiles are attributed to north and central coastal styles including some with Lambayeque iconography. Non-regional styles include Wari textiles with geometric iconography and one with discontinuous warp and weft tie-dye.

Chapter 4 Dye analysis & SERS

4.1 Dye Analysis

There are a number of challenges in analyzing dyes arising from the nature of the material. Both the low concentration of the dye and the strong affinity to the fiber render identification of dyes difficult. Their complex organic molecular structure inhibits analysis using some common analytical methods such as hand-held X-ray fluorescence spectroscopy (XRF), which is not sensitive to low atomic (Z) number elements such as aluminum (often found in mordant dyes), or x-ray diffraction spectroscopy (XRD), which requires a crystalline structure. Additionally, dye molecules can be severely altered by a number of means, such as the reducing environment induced by the decomposition of associated human remains, or photo oxidation from exposure to sunlight. Molecules may also undergo alteration during the extraction process usually required for analysis. Despite these difficulties, it is possible to extract dyes from textiles and identify the source based on their constituent chemical compounds. The most common techniques for this are high performance liquid chromatography (HPLC) coupled with mass spectrometry (MS) or ultraviolet-visible-spectrophotometry (UV-Vis), gas chromatography-mass spectrometry (GC-MS), thin layer chromatography (TLC) also coupled with mass spectrometry (LC-MS). These techniques utilize liquid extractions usually requiring a yarn sample of a few mm in length during which the fiber is digested by the extraction process. The benefit of the chromatographic techniques is their highly discriminating power, particularly when multiple dyes are used to color an individual yarn. While there are a number of advantages to these techniques, the sample size requirement can be a limitation, particularly when working with archaeological material.

4.2 Surface Enhanced Raman Spectroscopy (SERS)

Raman spectromicroscopy (μ RS) is a high accuracy, non-invasive, non-destructive analytical technique that uses light scattering to identify molecular vibrations in an analyte, revealing vital

information about its chemical structure and physical state [45]. This technique involves the irradiation of a sample with a high-intensity monochromatic radiation (laser beam) and the spectral analysis of photons inelastically scattered by the sample. The incident radiation induces an oscillating dipole, causing the analyte to scatter the majority of photons at the same frequency as the incident radiation without energy transfer, a phenomenon known as Rayleigh elastic scattering. Incident photons (approximately 1 out of every 10^{30} photons) can also interact with the molecules in a way that energy is either gained or lost causing a shift in frequency of the scattered photons (inelastic scattering). This inelastic scattering is also known as the Raman shift and depends on the polarizability of the molecules. The incident photon energy can excite vibrational modes of polarizable molecules, yielding scattered photons with lower energies equal to the amount of the vibrational transition energies. These energies are below the Rayleigh scattering peak at the incident frequency and are called "Stokes lines". It is also possible to observe weak scattering at frequencies above the incident frequency known as "anti-Stokes" lines.

Spontaneous Raman scattering is typically very weak and as a result difficult to detect.

Typically, the excitation beam is focused on a spot of $\sim 1\ \mu\text{m}$ diameter using an optical confocal microscope and backscattered photons are collected by the same microscope objective.

Inelastically scattered photons are sorted spectrally by a diffraction grating and detected by a photon-counting photomultiplier tube or, more commonly now, a CCD camera. The resulting spectrum, plotted as the photon intensity versus the wavenumber shift, provides information on the molecular composition and structure of the sample. As Raman spectroscopy is a "fingerprinting" technique, comparing their characteristic vibrational spectra with known spectra in a spectral library/database generally identifies materials.

Raman scattering can also be overwhelmed by naturally fluorescent organic materials, or by fluorophore contaminants. Numerous techniques have been developed to circumvent

fluorescence; among these, the long or short wavelength lasers used as excitation source [46] and the use of surface-enhanced Raman scattering (SERS), a surface-sensitive technique that helps quench fluorescence and increase significantly the signal-to-noise ratio. SERS Raman scattering occurs from molecules absorbed on the roughened surface of certain metal (normally silver or gold) substrates [47, 48] or specific nanostructured [48, 49] and microfluidic plasmonic platforms [50-52] achieving an enhancement factor up to 10^8 . Using a laser source with wavelength close to the SERS active-surface localized surface plasmon resonance (LSPR) wavelength, can achieve maximum SERS enhancement. At its strongest SERS enables vibrational fingerprinting down to the single molecule, though enhance in the range of 10^4 to 10^6 times is more typical [53]. It is generally accepted that major contributors to most SERS processes are electromagnetic and chemical mechanisms with the former being the most dominant [54-61].

4.3 SERS dye analysis

Although the technique was developed over 30 years ago, only in the previous decade was SERS exploited for the analysis of archaeological and cultural objects for the identification of pigments and dyes [54, 62-69]. The impetus for the adoption of SERS is its advantage of identifying molecules at low concentrations using reduced sample sizes. In recent years, SERS dye research has improved and expanded methodologies to include application of variety of dye molecules, to confront analytical challenges, and develop minimally invasive and noninvasive methodologies. Studies have included chemical standards and reference dyes extracted from textiles, as well as historical and archaeological textiles.

4.3.1. SERS techniques and advances

A number of methods for synthesizing and incorporating SERS-active metals have been utilized in dye analysis, the most common platform being silver nanoparticle (AgNPs). AgNPs can be formed and applied as nanoisland films [70, 71] though also commonly synthesized and applied

as a colloid. There are a number of procedures for synthesizing colloids, including microwaving silver with sulfuric acid [63] and photoreduction using laser irradiation [72, 73]. The most common synthesis is the Lee & Meisel method in which nanoparticles are reduced from silver nitrate using sodium citrate (used in this study) or sodium borohydride [74]. Its performance is improved when centrifuged for concentration to form what is referred to as a colloidal paste [75]. There are benefits and detriments to each synthesis method, and studies have been dedicated to comparing their performances [76, 77]. Citrate reduced AgNPs are among the most stable due to the absorption of citrate on their surface, which also acts as a buffer maintaining about 6.5 pH. While their stability and ease of preparation are benefits, the analyte molecules must compete with their strong affinity to the surface of the AgNPs, and interference bands from the citrate are common [76].

A variety of extractions may be employed for dye analysis using SERS, including liquid, gel, and in situ methods. Some are variations on extractions used for HPLC, including liquid hydrolysis with hydrochloric acid in methanol [62, 70] and chelation using EDTA to extract mordanted dye using either liquid or gel [47, 78]. With in situ extraction, the analyte is detached from the fiber substrate though remains on the surface. The best example of this is the hydrofluoric (HF) vapor micro-chamber extraction [47, 65, 71, 79]. To perform this extraction, a dyed fiber segment is exposed to HF vapors from a drop of HF in a small capsule chamber, after which it is coated with AgNPs and analyzed. While effective, this method has limitations due to the toxicity of HF. Researchers have also had success using in situ extractionless methodologies using both reference and historical fiber samples [72, 75, 80, 81].

In addition to developments in SERS substrates and extraction methods, SERS dye analysis has included other technological advances. This includes preparing samples with UV-laser ablation prior to analysis [82]. SERS has also been improved by coupling with additional analytical equipment, including coupling with thin layer chromatography for further identification

of the analyte [80] or with scanning electron microscopy (SEM), which has shown improved visualization of sample and AgNPs aggregation and greater spatial resolution [83, 84]. SERS combined with density functional theory (DFT) analysis has also been applied to gain better understanding of the interaction between the analyte and AgNPs on a fundamental level [85].

4.3.2. Applications of SERS for the identification of cochineal and *Relbunium*

The effectiveness of SERS is dependent on the geometry, functional groups, formal charge or dipole, and the effect of pH on the analyte, which will determine its affinity for the nano-rough metallic substrate and the mechanisms for adsorption. Because of this, some compounds are more readily analyzed using SERS than others. Molecules such as alizarin have multiple potential mechanisms and orientations for adsorbed on the surface of the AgNPs, which eases analysis because of the increases in potential for interaction between the analyte and AgNPs [76]. A number of dye molecules have been analyzed with this technique, including the anthraquinone dyes carminic acid, purpurin, and alizarin. Recently, pseudopurpurin was also identified using SERS, which is the primary coloring compound of *Relbunium* [14]. The spectrum of anthraquinones is pH dependent, and a number of studies are dedicated to identifying different anthraquinone standards at different pH levels.

Chapter 5 Materials and Methods

5.1 Sample materials

5.1.1. Chemical standards and reference materials

Chemical standards of carminic acid (Fluka, Sigma-Aldrich 11298 analytical standard), purpurin (Fluka, Sigma-Aldrich 82631 Standard Fluka) and alizarin (Sigma-Aldrich 122777 97%) were diluted in ethanol (Product info) to a 0.001M solution. Chemical standard of pseudopurpurin is not commercially available, so a chemical standard was obtained from a wool yarn dyed with pure pseudopurpurin from the Helmut Schweppe collection held by the Getty Conservation

Institute, provided by LACMA. To analyze this chemical standard, the dye was extracted using the HF method described below in 5.4.1. Both unmordanted and alum mordanted wool reference fibers dyed with cochineal, *Relbunium ciliatum*, and *Relbunium hypocarpium* were acquired from the Max Saltzman collection held by the UCLA/Getty Conservation Program.

5.1.2. Archaeological materials

Seven archaeological red yarn samples were analyzed, all of which were sampled by archaeologist Rommel Ángeles Falcón from seven textiles housed in the Museo Municipal Huaca Malena in Capilla de Asia, Peru. All archaeological samples are camelid fibers from red dyed weft, as discussed below in the characterization section. Two of the samples are from Wari style textiles, while the others are Malena style, as designated by Ángeles Falcón.





Figure 1. TOP ROW (Images and information courtesy of Rommel Ángeles Falcón) A (sample VM01): camelid warp and weft bag, eccentric tapestry technique, mountain style; B(sample T-130A): cotton warp and camelid weft band, eccentric tapestry technique, Wari style; C (sample VM04): undyed cotton and dyed camelid polychrome band, double weave technique; D (sample 061.02.01): camelid, tapestry technique, Wari/Malena style. BOTTOM ROW (information courtesy of Rommel Ángeles Falcón): E (sample T-69): cotton warp camelid weft cloth, slotted tapestry technique, Malena style; F (sample 77.10.02):, cotton and camelid corner of cloth, brocade technique, Malena style; G (sample 119.000.029): camelid warp and weft uncu fragment, eccentric tapestry technique, Wari style.

5.2 Microscopy and image analysis

5.2.1. Optical microscopy of fiber samples

Archaeological fiber samples were imaged using a Keyence VHX-1000 digital optical microscope and an Olympus BX51 polarized light microscope. A Nikon D90 SLR camera was used to record the digital images from the Olympus BX51 microscope. Before imaging, both the yarn and individual fibers were rinsed in ethanol, and for transmitted light, samples were placed in a drop of water on a glass slide with a glass cover slip.

5.2.2. Scanning electron microscopy of fiber samples and AgNPs

AgNPs and archaeological fiber samples were imaged using the FEI Nova NanoSEM230™ variable pressure (VP) scanning electron microscope (SEM) at high vacuum using a secondary electron detector. AgNPs were pipetted onto a SEM stub and allowed to dry. Fiber samples were imaged without pre-treatment and after rinsing with ethanol to remove debris from the surface. The fiber samples were then gold coated using an Anatech Hummer 6.2 sputtering system under vacuum to enhance conductivity for higher resolution imaging.

5.2.3. Image analysis of fiber samples and AgNPs

Microscopy images were measured to scale using ImageJ to acquire accurate diameter measurements. Fifty FWHM (full width at half maximum) diameter measurements were taken on AgNPs from SEM images. The diameters of archaeological fibers were measured from digital microscope images by averaging measurements from fifteen different fibers taken from areas where they were in focus in the image to increase accuracy.

5.3 Fiber optic reflectance spectroscopy (FORS) of AgNPs and archaeological samples

Absorbance of the AgNP stock batch was characterized using an ASD Inc. Fieldspec® 3 spectrometer⁸ with range of 350 nm to 2500 nm range and a high intensity contact probe (spot size: $\varnothing \sim 10$ mm), operating in reflectance mode. 3 ml of stock batch AgNPs was pipetted into a petri dish, which was placed on a white background and with the spectrometer held just above the surface of the colloidal solution. The light passed through the solution, was reflected by the white background and passed again through the colloidal solution. The archaeological samples were characterized using an Ocean Optics 2000+ Miniature Fiber Optic Spectrometer with QR400-7-UV-VIS reflection probe with 0.4mm diameter and HL 2000 halogen light source with 2° observer angle for data collection between 400-700 nm⁹. The yarn samples were placed on a white background and care was taken to cover as much of the spot size with the width of the yarn sample.

5.4 Surface Enhanced Raman Spectroscopy (SERS)

5.4.1. Sample preparation

Individual fiber samples were carefully removed for analysis from yarn samples of the Schweppe (pseudopurpurin) and Saltzman (cochineal and *Relbunium*) collections and from

⁸ This instrument has a spectral resolution of 3 nm at 700 nm and 10 nm at 1400/2100 and measurements were calibrated with a white Spectralon (PTFE) standard

⁹ This instrument has a detector range of 200-100 nm and calibrated with WS-1 reflectance standard using standard illuminant D65 (daylight) setting.

archaeological yarn samples ranging approximately from 1 mm to 5 mm in length. The archaeological samples were rinsed using a drop of ethanol prior to further preparation steps. The dyed fibers were subsequently analyzed using one of the following pre-treatment methods: 1) extractionless on-the-fiber analysis); 2) in situ on-the-fiber HF vapor micro-extraction, 3) on-the-fiber micro-extraction with formic acid in ethanol and 4) on-the-fiber liquid micro-extraction using HCl in methanol and water. For extractionless preparations, an individual fiber was taped to an SEM stub with copper tape. The sample was then coated in AgNPs and analyzed directly on the fiber as described below.

The micro-extraction using HF vapors was conducted in a micro-chamber capsule containing HF in which the fiber is exposed as described by Leona [71]. Pre-treatment using HF micro-extraction was carried out at the LACMA Conservation Science lab. A 20 μ l drop from HF (Sigma-Aldrich, 48% w/v in water, $\geq 99.99\%$ purity) was pipetted into a conical micro chamber (Ted Pella 130 size 00). An individual sample fiber was cut into three small segments each approximately 1-2 mm, placed in a smaller capsule cap (Ted Pella 130-B size 3) and inserted horizontally into the chamber. Samples were exposed to HF vapors for 5 minutes and subsequently removed. Following the micro-extraction, the fibers were coated with AgNPs and analyzed directly.

Formic acid (CH_2O_2) was used for dye extraction, similarly to recent studies [80, 86]. A 25% (pH 1.5-2.0), solution of formic acid (EMD Chemicals FX0440-5 98%) in ethanol (J.T. Baker for Histological use A.C.S. Reagent 94.9% denatured ethanol, 5% isopropanol) was prepared ahead of time. An individual fiber segment was placed on an SEM stub and 2 μ l of the solution was applied to the sample in 1 μ l drops, which were allowed to dry between applications taking approximately 2 minutes. Once dry, AgNPs were deposited over the fiber and analyzed both on and off the fiber.

A liquid extraction solution using HCl was prepared as described for HPLC and SERS applications [5, 70]. 37% HCl (Sigma-Aldrich 258148 A.C.S. reagent) was combined with methanol (Sigma-Aldrich 322415 99.8%) and ultra-distilled water in a 2:1:1 ratio. Samples segments of individual fibers approximately 2mm long were placed at the bottom of a conical micro-capsule (Ted Pella 130-B) and covered with 50 μ l of the solution. The samples were left to soak for an hour and a half, then placed in test tubes and put into a hot water bath at 100°C for 10 minutes with glass beads to prevent the test tubes from touching the bottom. The solution was pipetted 10 μ l at a time onto cleaned glass slides on a warm hot plate. Once the liquid was dry, another drop was placed in the same location. Chemical standards were prepared for comparison by combining 10 μ l of 0.001M dye solution in ethanol with 20 μ l solution of HCl:MeOH:H₂O in a 2:1:1 ratio. The mixture was dispensed onto a cleaned glass slide and allowed to dry on a warm hot plate. Both fiber and chemical standard samples were prepared in advance and within the following days, samples were then coated with AgNPs and analyzed.

5.4.2. Synthesis of Silver nanoparticles (AgNPs)

AgNPs were synthesized using the Lee and Meisel method [74]. 18 mg of anhydrate silver nitrate powder (Sigma Aldrich product 20139 ACS reagent 99+%) and 100 ml of ultra-distilled water (Millipore Milli-Q plus system(R \geq 18.2 M Ω .cm) were combined with 22.4 mg of sodium citrate dehydrate (Fisher Science Education S25545 Lab Grade) in a 1% solution upon boiling. The sodium citrate was introduced using a programmable syringe pump over the course of one minute to induce rapid nucleation and ensure smaller particle size and distribution [87]. After an hour of boiling, either covered or using a condenser, the flask was submersed in an ice water bath to prevent particle growth during cooling [88, 89]. The stock batch of AgNPs was centrifuged 6 ml at a time using a Fisher brand miniature centrifuge for 10 minutes at 6400 rpm. The condensed particles were then combined into one vial to less than 0.05 ml. Centrifuged

batches generally lasted about four to six weeks before expiring, though some batches expired within one to two weeks. The cause of this discrepancy is unknown.

5.4.3. SERS and Raman spectromicroscopy

0.5 μl of AgNPs was deposited onto the fiber followed by 0.5 μl of 0.2M KNO_3 (Alfa Aesar A14527 99%). After five minutes, the excess colloid and KNO_3 was removed with a KimWipe (Kimberly-Clark Corp)¹⁰. For samples prepared using the liquid HCl extraction, this extra step was not necessary, and instead, the remainder of the liquid quickly evaporated under the light of the objective. After the 5-minute drying period, the samples were analyzed at UCLA using a Renishaw inVia Raman spectrometer with 785 nm and/or 633nm lasers and Leica confocal microscope interface with 50x objective. Samples extracted using HF vapor followed the same procedure for application of AgNPs, and were analyzed using a Chromex Senturion (now Bruker, Billerica, MA) Raman spectrometer with 785 nm laser and Olympus LMPlan 20x objective.

¹⁰ Using a KimWipe also helped prevent crystallization of KNO_3 on the sample, which can generate signals in SERS spectra.

Chapter 6 Results and Discussion

6.1 Characterization of AgNPs

The AgNPs used in this study had a maximum wavelength of energy absorption at approximately 400 nm as determined by visible-range fiber optics reflectance spectrophotometry (Vis-FORS). Their average FWHM (full width at half maximum) diameter ranged from 50-65 nm [69], as measured in ImageJ using SEM images (Table 2). The particles had a range of sizes and shapes, with most being slightly faceted and oblong though rods and wires were also present (Figure 2); all of which are consistent with expectation for AgNPs synthesized using the Lee and Meisel method. μ RS of the aggregated colloid showed broad bands at 1300 cm^{-1} , 1600 cm^{-1} , a sharp peak around 1050 cm^{-1} (due to KNO_3 used to aggregate the AgNPs), and a wide band near 500 cm^{-1} . These results were consistent for multiple AgNPs batches. When analyzing dye samples, the Raman signal associated with the AgNPs was overwhelmed by the analyte. Though in many spectra, the prominent peak at 1050 cm^{-1} still occurred. As the concentrated batch of AgNPs began to age (photo degrade), sharper peaks in the region between 800-1400 cm^{-1} were observed (Figure 3) [77]. When these interference bands occurred, the colloid was considered expired and a new batch was centrifuged or synthesized. To prevent degradation, AgNPs were stored in a cool place and wrapped in metal foil.

Full Width at Half Height Measurements				
Batch	Average	Minimum	Maximum	StDev
1	64.977	41.261	108.301	16.199
2	49.423	31.602	31.602	10.990

Table 2. Full Width at Half Height measurements of two batches of silver nanoparticles used in this study

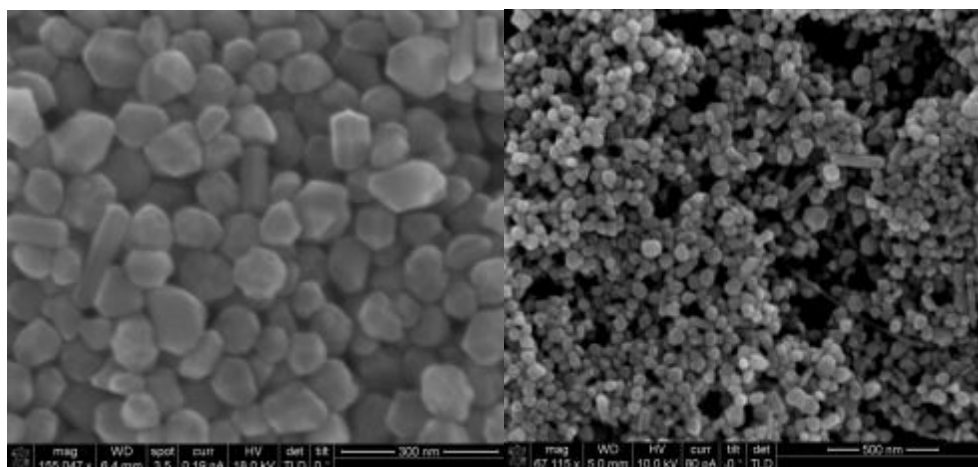


Figure 2. Secondary electron micrographs of AgNPs. Two different batches of AgNPs (right micrograph: Yuan Lin 2015) displaying round faceted particles along with rods (left image) and some wires (right image).

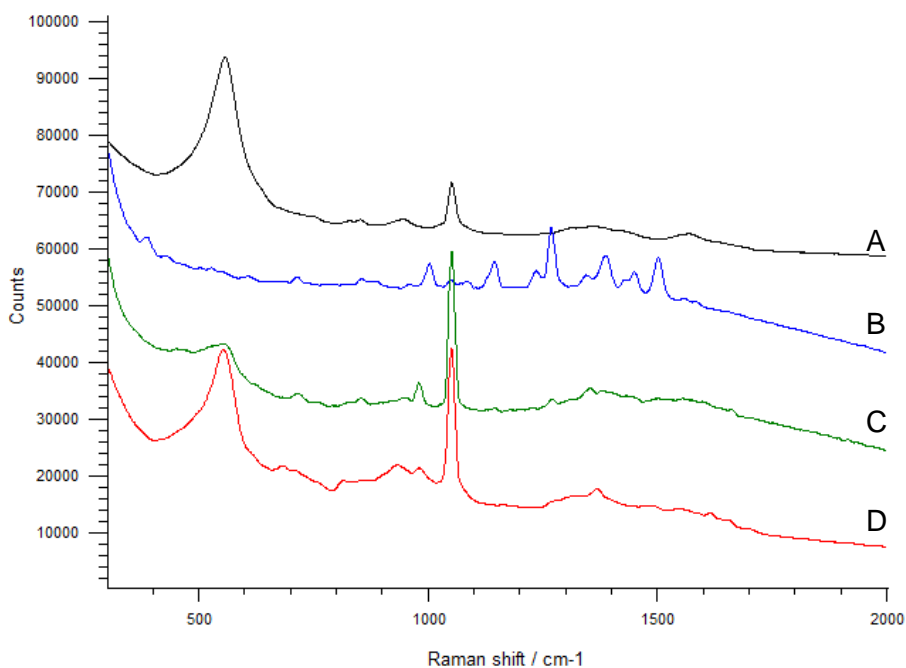


Figure 3. Raman spectra of centrifuged batch 1 AgNPs analyzed within the first few days after synthesis (A) compared to the same expired batch analyzed three months later (B). Both spectra were acquired using a 785nm laser at 0.25% laser strength for 10 seconds and 1 acquisition after using KNO_3 to aggregate AgNPs. Raman spectra of centrifuged batch 2 AgNPs analyzed within the first few days after synthesis (C) compared to the same batch analyzed one month later (D). Both spectra were acquired using 633nm laser at 0.25% laser strength for 10 seconds and 1 after using KNO_3 to aggregate AgNPs. The large peaks at 1050 cm^{-1} are due to the KNO_3 added to the AgNPs.

6.2 Characterization of archaeological textiles and fiber type

6.2.1. Fiber and yarn type

All samples are spun in Z direction and plied with two threads in the S direction. Yarns constructed in this manner are typical of both highlands and the central and southern coastal regions, whereas, Z(2S) thread is typical of the north coast [90, 91]¹¹. Based on the fiber diameter, the morphology of the medulla and cortex features, all archaeological samples are characterized as camelid fibers (Table 3). Camelid fibers are distinguished by the presence of a straight smooth profile, an irregular shaped medulla both continuous and interrupted, and an indistinct cuticular scale pattern known as irregular waved mosaic [92]. The fineness of the fibers both in diameter and scale pattern and the presence or absence of guard hairs are further distinguishing features between different species of camelid both domesticated (alpaca and llama)¹² and wild (vicuña and guanaco)¹³ [93]. However, the fleece of ancient domesticated species were likely more homogenous than those of today due to interbreeding of domesticated species after post Spanish conquest [92]. Additionally, the diameter of fibers can vary greatly depending on factors such as where in the coat the fibers originated and the age of the animal. All these factors make distinguishing between species of camelid challenging. While camelid fibers are morphologically similar to human hair, human hair averages about 90µm of thickness [93].

¹¹ Ply/spin notation follows method used in the referenced study on textiles from Huaca Malena, where the first letter designates the ply direction, and the number and letter in parenthesis designates the number of threads and their spin direction, based on the notation of Jeffrey Splitstoser (2012)

¹² Llama fibers have a higher percentage of guard hairs compared to alpaca, though both have diameters ranging from 10-60µm an average 26-28 µm

¹³ Guanaco average diameter between 18 to 25 µm, 10-11 scales per 100 µm

Sample	Construction attributes				Fiber Diameter (μm)			
	Motif style	Orientation	Ply(Spin)	Fiber Type	Average	StDev	Minimum	Maximum
VM01	Malena	weft	S(2Z)	camelid	28.07	7.62	16.87	42.46
T-130A	Wari	weft	S(2Z)	camelid	18.66	3.99	9.88	23.12
VM04	Malena	weft	S(2Z)	camelid	25.69	4.40	21.20	35.29
61.02.01	Malena	weft	S(2Z)	camelid	28.64	5.37	21.96	43.70
T-69	Malena	weft	S(2Z)	camelid	30.71	9.50	19.98	51.31
77.10.02	Malena	weft	S(2Z)	camelid	28.10	8.64	18.60	45.40
119.000.029	Wari	weft	S(2Z)	camelid	28.74	5.85	17.57	38.69

Table 3. Ply/spin notation follows method used in other studies on textiles from Huaca Malena, where the first letter designates the ply direction, and the number and letter in parenthesis designates the number of threads and their spin direction. Fiber diameter measurements, taken from 15 data points were acquired from photomicrograph of a yarn and measured in ImageJ.

Most of the samples are comparable in average fiber diameter and consistent to those reported for camelid species. The largest fiber average diameter (in sample T-69) includes a guard hair. T-130A fibers are considerably finer than the other sample and may represent an adolescent of an ancient domesticated species as it is within the range of contemporary industrial standards for baby alpaca.¹⁴ The diameter average and range is also comparable to wild vicuna however these fibers are very rare and tan in color. For more in depth characterization of these fibers, further investigation into the morphology and diameter is required.

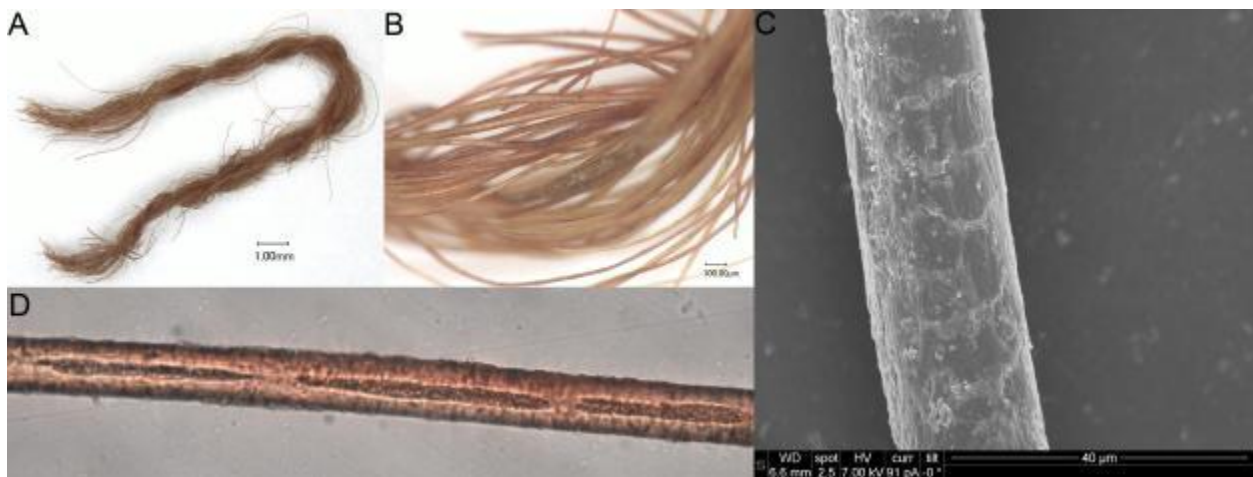


Figure 4. VM 01 photomicrographs: yarn samples images with digital microscope (A-B), cuticular scale pattern imaged with SEM (C), and interrupted medulla imaged with transmitted light (D).

¹⁴ http://islandalpaca.com/about_alpacas.php

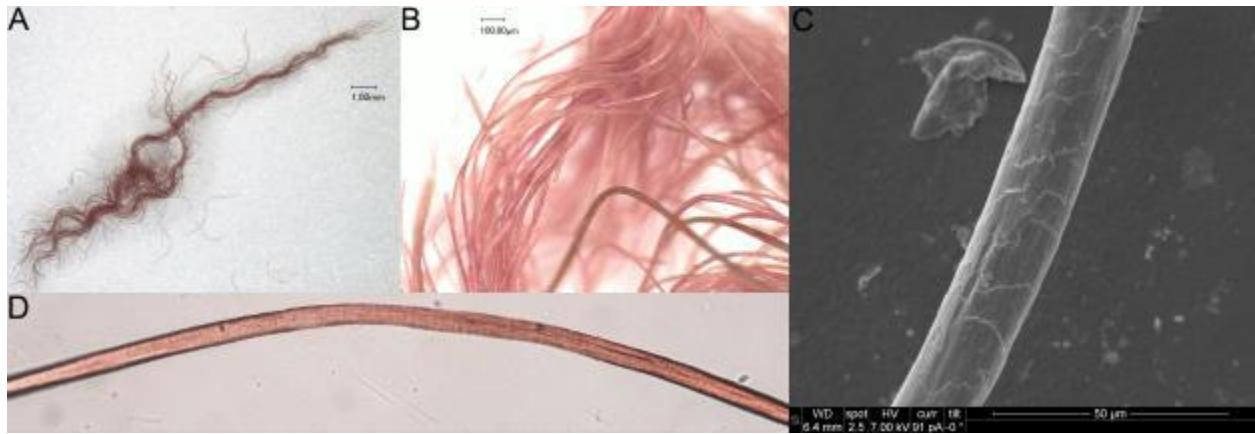


Figure 5. T-130A photomicrographs: yarn samples images with digital microscope (A-B), cuticular scale pattern imaged with SEM (C), and interrupted medulla imaged with transmitted light (D).

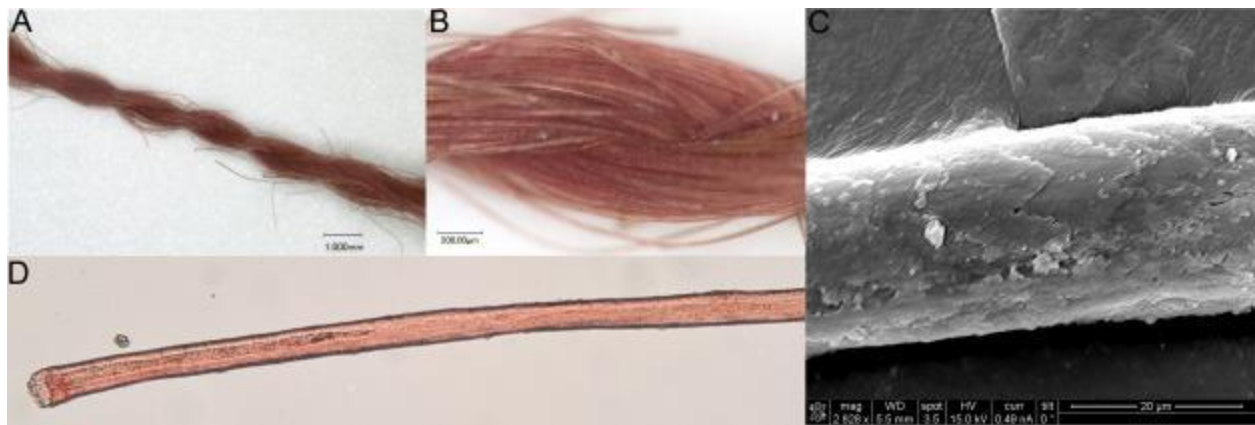


Figure 6. VM 04 photomicrographs: yarn samples images with digital microscope (A-B), cuticular scale pattern imaged with SEM (C), and interrupted medulla imaged with transmitted light (D).

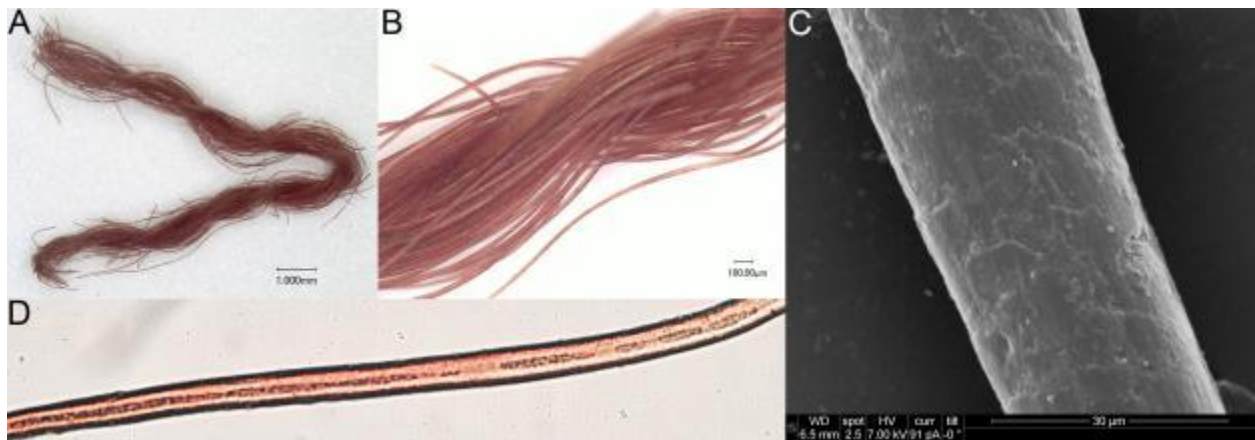


Figure 7. 061.02.01 photomicrographs: yarn samples images with digital microscope (A-B), cuticular scale pattern imaged with SEM (C), and interrupted medulla imaged with transmitted light (D).

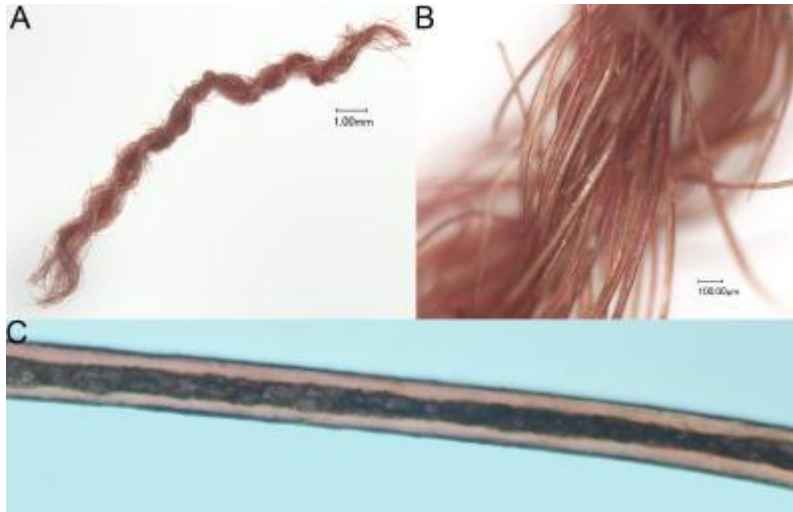


Figure 8. T-69 photomicrographs: yarn samples images with digital microscope (A-B) and uninterrupted medulla imaged with transmitted light (C).

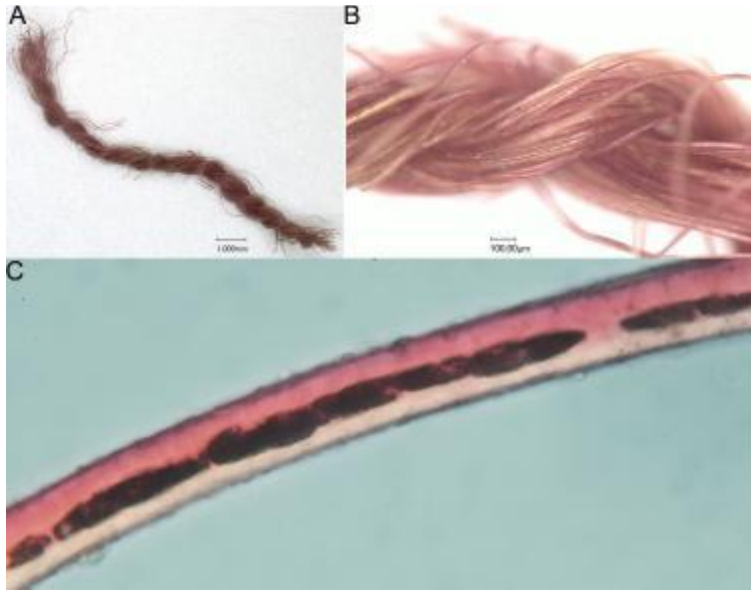


Figure 9. 77.10.02 photomicrographs: yarn samples images with digital microscope (A-B) and interrupted medulla imaged with transmitted light (C).

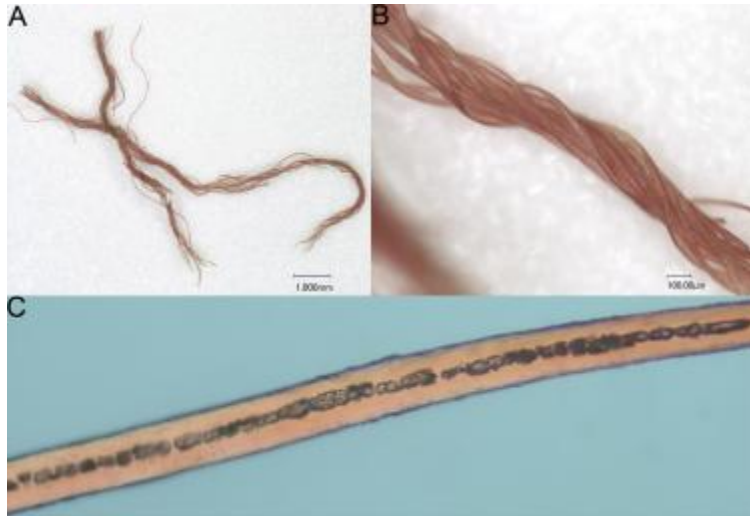


Figure 10. 119.000.02 images: digital microscope (top) and transmitted light image of interrupted medulla (bottom).

6.2.2. Condition of archaeological fibers

The condition of the fiber samples was evaluated using digital microscopy, polarized light microscopy in transmitted light and SEM. All samples are heavily covered with burial contaminants. Rinsing the yarn samples in ethanol appears to remove part of the debris, though even with rinsing there are still residual particulates (Figure 11). The presence of contaminants was also evident with SERS analysis, where distinct spectra of unknown origin were consistently found in the archaeological samples, even after rinsing in ethanol.

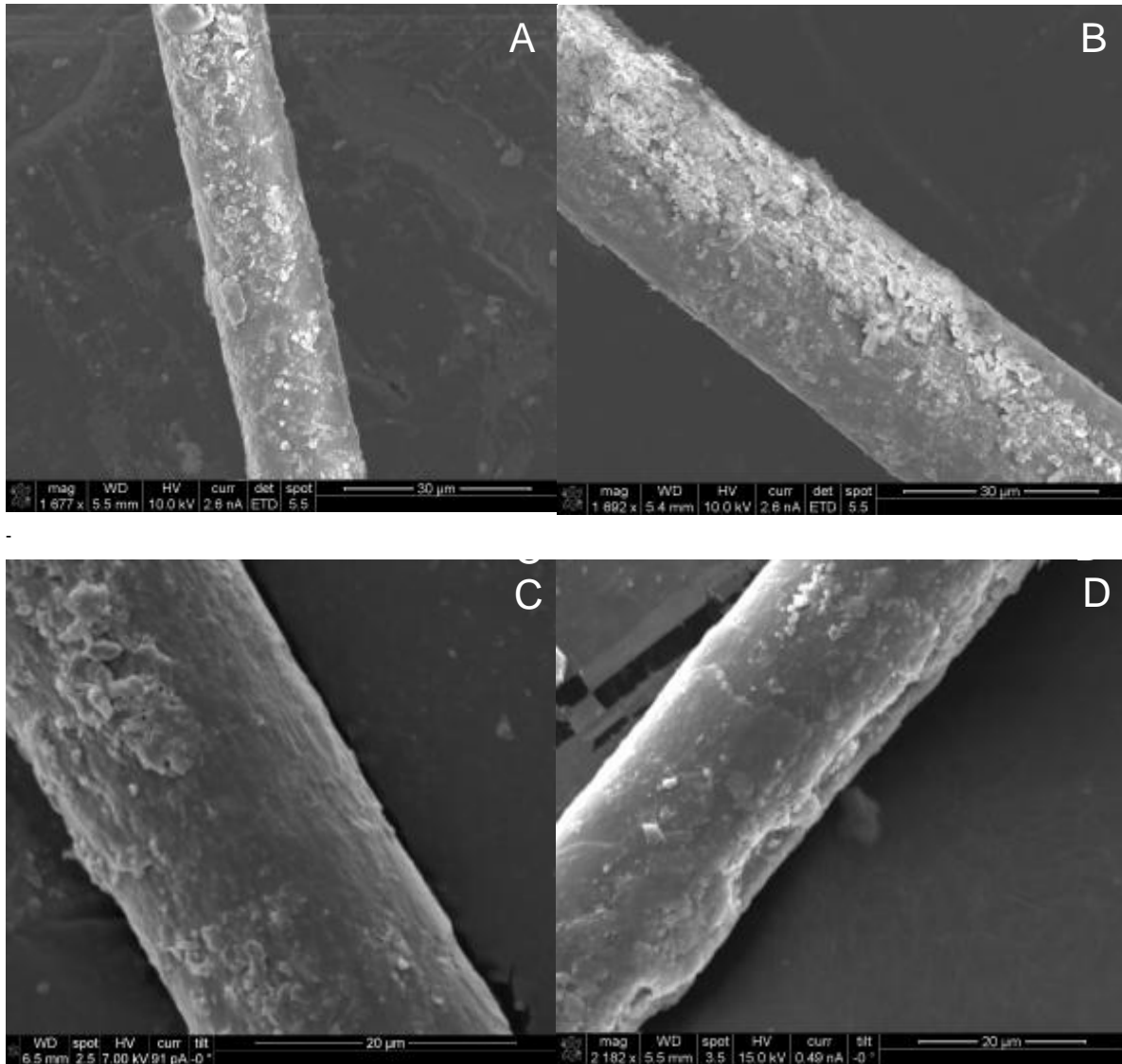


Figure 11. Secondary electron micrographs of archaeological samples covered in burial contaminants both before rinsing in ethanol (A-B) and after rinsing (C-D) of VM03 (A), T-130A (B), VM01 (C) and VM04 (D).

The fibers themselves also show patterns of degradation. The individual fibers are very brittle, with physical damage (breaks, cracks) visible in all samples (Figure 12). Fibers from sample T-130A include evidence of deterioration (creasing and folding) normally caused in alkaline environments (Figure 13) [93]. Alkaline environments, known to degrade proteinaceous fibers [94], are common in burials due to the decomposition of human remains. Deterioration caused

by elevated pH is likely to impact the dye as well as the substrate. Other physical deterioration as for example twists and splitting are also observed in the archaeological fibers (Figure 14).

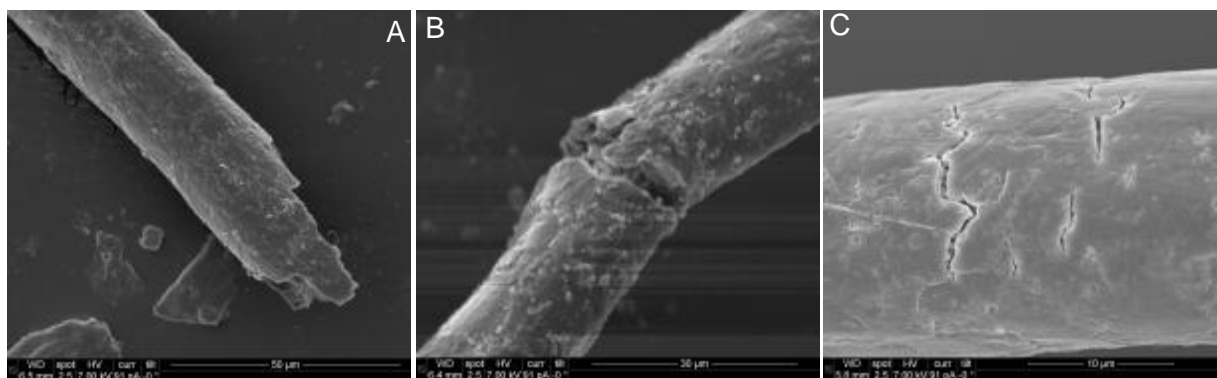


Figure 12. SEM images of VM01 (A) T-130A (B) and VM04 (C) showing cracking and breaking in the brittle fibers.

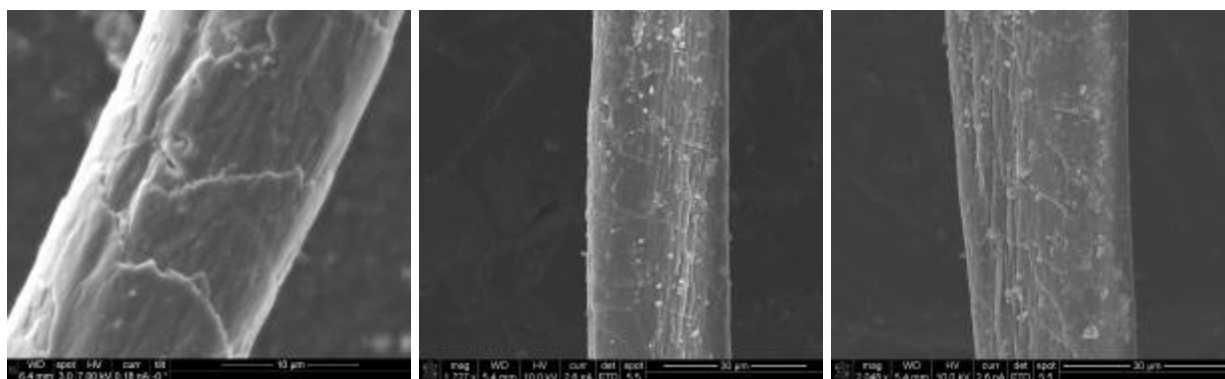


Figure 13. Secondary electron micrographs of fibers from sample T-130A, displaying crease and folds in the fiber, perhaps do to exposure to an alkaline environment during burial.



Figure 14. Transmitted light images of T-69 and 77.10.02 displaying distortion and splitting.

6.3 Characterization of reference dyes using SERS

Results of the analysis of chemical standards for carminic acid [95], pseudopurpurin [14], purpurin[62, 70], and alizarin [68, 70, 96] were comparable to those in the published literature.

These standards were used for identification of specific molecules in reference materials from the Saltzman collection dyed with cochineal and *Relbunium* (see 5.1.1.), which were analyzed using different extraction methods for SERS analysis. The following subsections include the results SERS data acquired from these extractions methods tested on reference fibers from the Saltzman collection.

6.3.1. Extractionless on-the-fiber SERS

Using on-the-fiber analysis without extraction unmordanted cochineal dyed fiber provided results comparable to those of carminic acid under non-acidic conditions (Figure 15). Using the same technique, unmordanted *Relbunium* dyed reference fibers match those of purpurin under non-acid conditions (Figure 16). As discussed above, pseudopurpurin is the predominant anthraquinone in *Relbunium*, though it is known to readily decompose to purpurin. While both molecules may be present in the sample, the proportion of purpurin may be higher or experiment conditions may be more favorable for detection of purpurin. For both cochineal and *Relbunium*, data was difficult to obtain and inconsistent between spots on the same sample.

Using this method, mordanted reference fibers of neither cochineal nor *Relbunium* yielded any results, suggesting that analysis of mordanted samples at a neutral pH without extraction is less effective when the dye is strongly bonded to fiber. Other studies have effectively analyzed mordanted fibers without extraction, and further testing may provide additional results [72, 75, 80, 81].

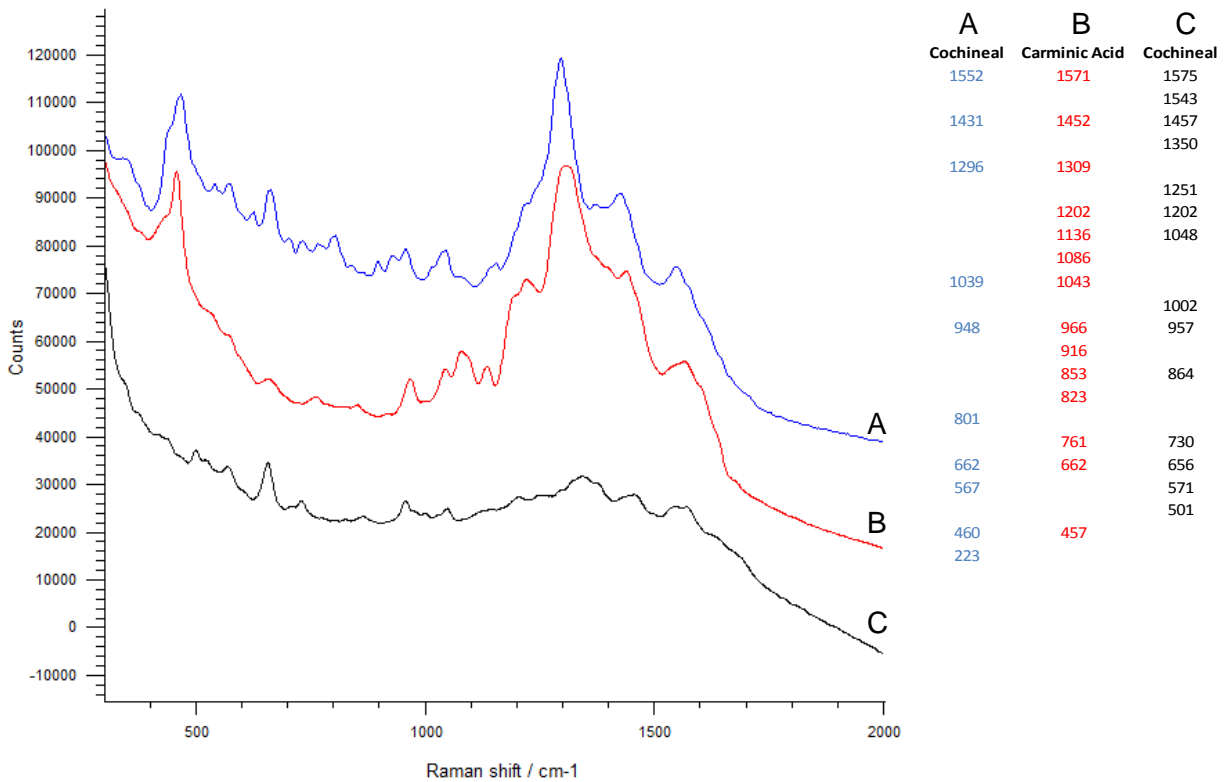


Figure 15. Raman spectra of on-the-fiber analysis without extraction on unmordanted (A) and mordanted (C) cochineal reference fiber, and 0.001M carminic acid in ethanol (B). Spectra were acquired using 785nm laser at 0.25% for 10 seconds at UCLA. Unmordanted cochineal spectrum (A) courtesy of Diana Rambaldi, acquired at LACMA using 785nm laser at 1% for 5 sec with 3 accumulations.

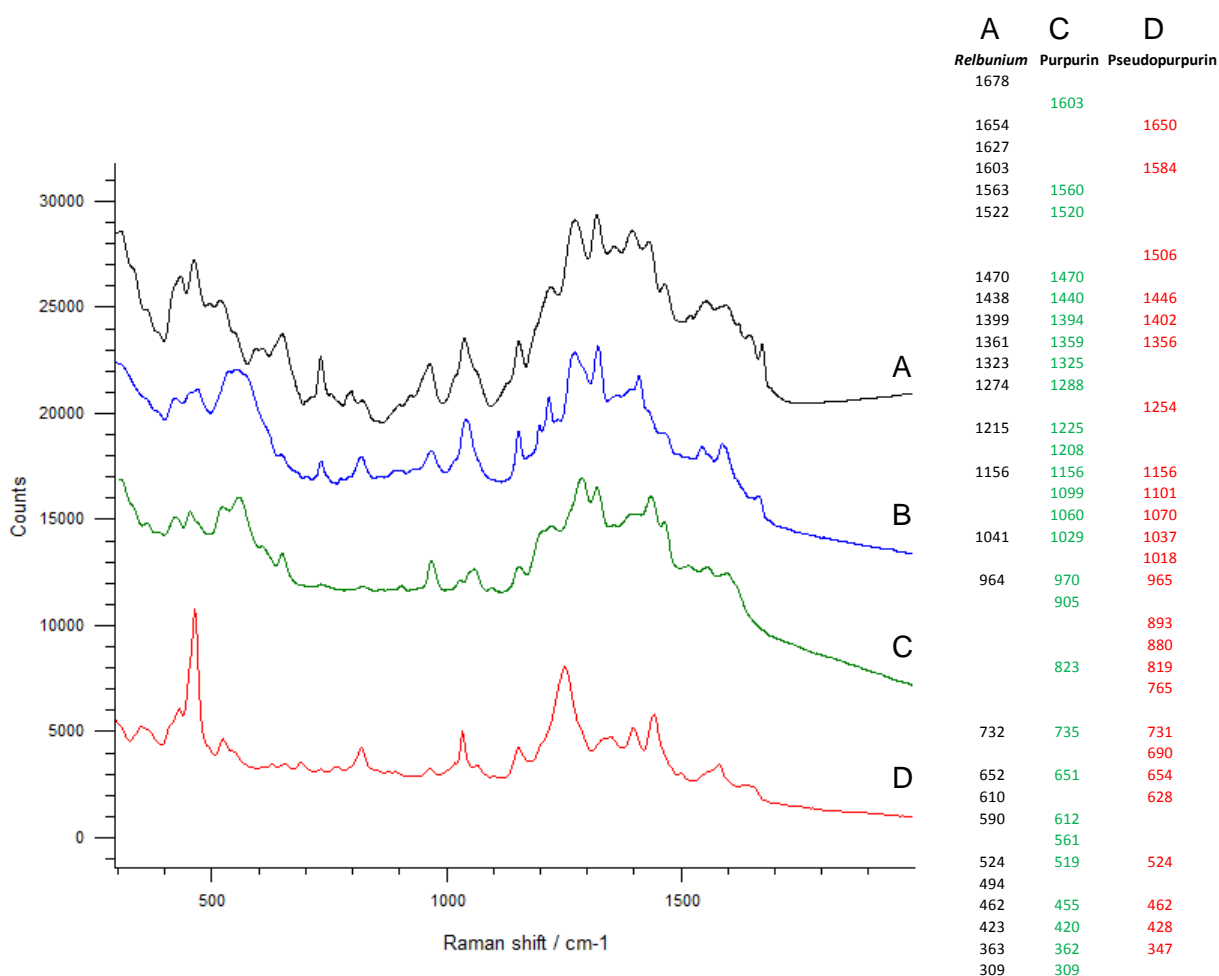


Figure 16. Raman spectra of on-the-fiber analysis without extraction of unmordanted *Relbunium hypocarpium* reference fibers (A and B) compared to purpurin (C) and pseudopurpurin (D). *Relbunium* samples (A and B spectra) acquired using 785nm laser at 0.05% for 10 sec at UCLA. Purpurin (C) acquired using 785nm laser at 0.25% for 10 sec at UCLA. Pseudopurpurin (D) was acquired at LACMA using 785nm laser at 1% for 5 sec.

6.3.2. On-the-fiber SERS with HF micro-extraction

On-the-fiber analysis using HF micro-extraction provided clear match between unmordanted cochineal and carminic acid under acidic conditions (Figure 17). The same technique provided a clear match between pseudopurpurin and *Relbunium* for both mordanted and unmordanted reference samples (Figure 18). Interestingly, purpurin does not contribute to these spectra as seen without extraction (Figure 16). Pseudopurpurin is a more acidic molecule than purpurin and the acidic conditions of this extraction method may therefore be more favorable for its

detection over purpurin. Pseudopurpurin is known to degrade to purpurin in highly acidic conditions as seen in strongly acidic liquid extraction methods [5], though this has not occurred using HF extraction method.

Results were more readily achieved from unmordanted samples versus mordanted, though sharp and consistent spectra were acquired from both samples. However, due to health and safety regulations using HF, this method was discontinued before mordanted cochineal could be included in this study. Instead, research focused on exploring less toxic extraction methods.

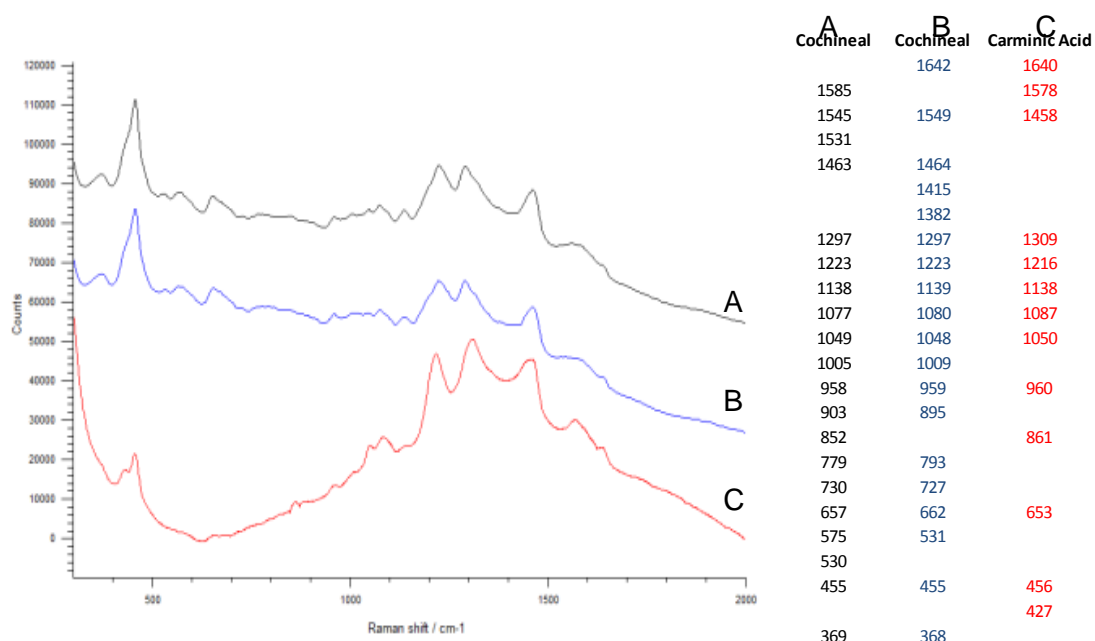


Figure 17. Raman spectra of HF micro-chamber extraction of unmordanted cochineal reference fibers (A and B) compared to 0.001M carminic acid combined with 5%HCl (C). Cochineal samples (A and B) acquired at LACMA using 785nm laser at 1% for 5 sec with 5 co-adds. Carminic acid (C) acquired using 785 nm laser at 0.25% for 10 sec at UCLA.

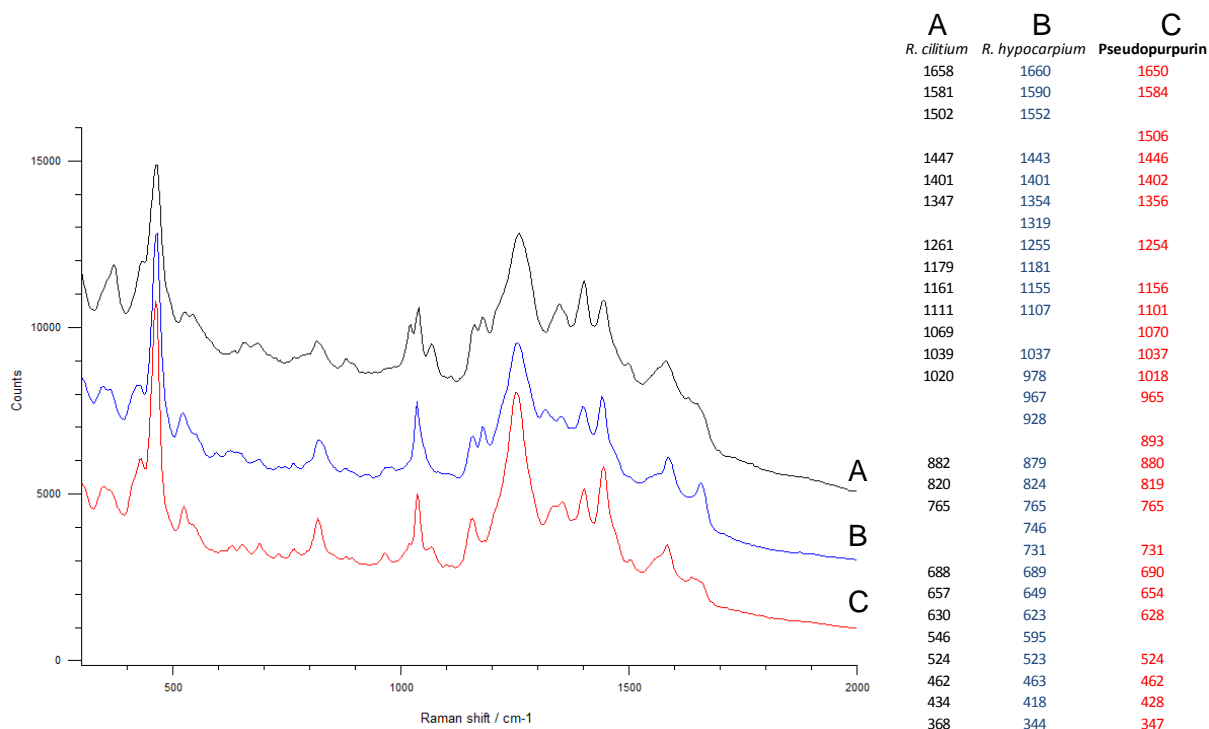


Figure 18. Raman spectra of HF micro-chamber extraction of *Relbunium* reference fibers mordanted *R. ciliatum* (A) and unmordanted *R. hypocarpium* (B) compared to pseudopurpurin (C) reference fiber extracted using the same technique. All spectra obtained using 785nm laser at LAMCA, A and C: 1% for 5 sec, B: 1% for 5 sec with 5 co-adds.

6.3.3. On-the-fiber SERS with formic acid micro-extraction

On-the-fiber SERS using 25% formic acid in ethanol micro-extraction of the mordanted cochineal sample provided a spectrum that matched that for the carminic acid chemical standard that was analyzed under non-acidic conditions (Figure 19). Similar results were also obtained from areas that contained formic acid in ethanol around the fiber on the glass substrate. This indicates this preparation method was successful at extracting carminic acid from the mordanted fiber. However as with cochineal samples analyzed without extraction, the molecule is consistent with carminic acid at a neutral pH.

The primary molecule detected when 25% formic acid was used to extract *Relbunium* from reference fibers was pseudopurpurin, however, the peak around 1349 cm^{-1} is very prominent

compared to the peak at 1356 cm⁻¹ observed in the pseudopurpurin standard (which was extracted from fiber using HF)(Figure 20). Overall, data were not readily reproducible using this technique, and it was more conducive to analysis of cochineal than *Relbunium*.

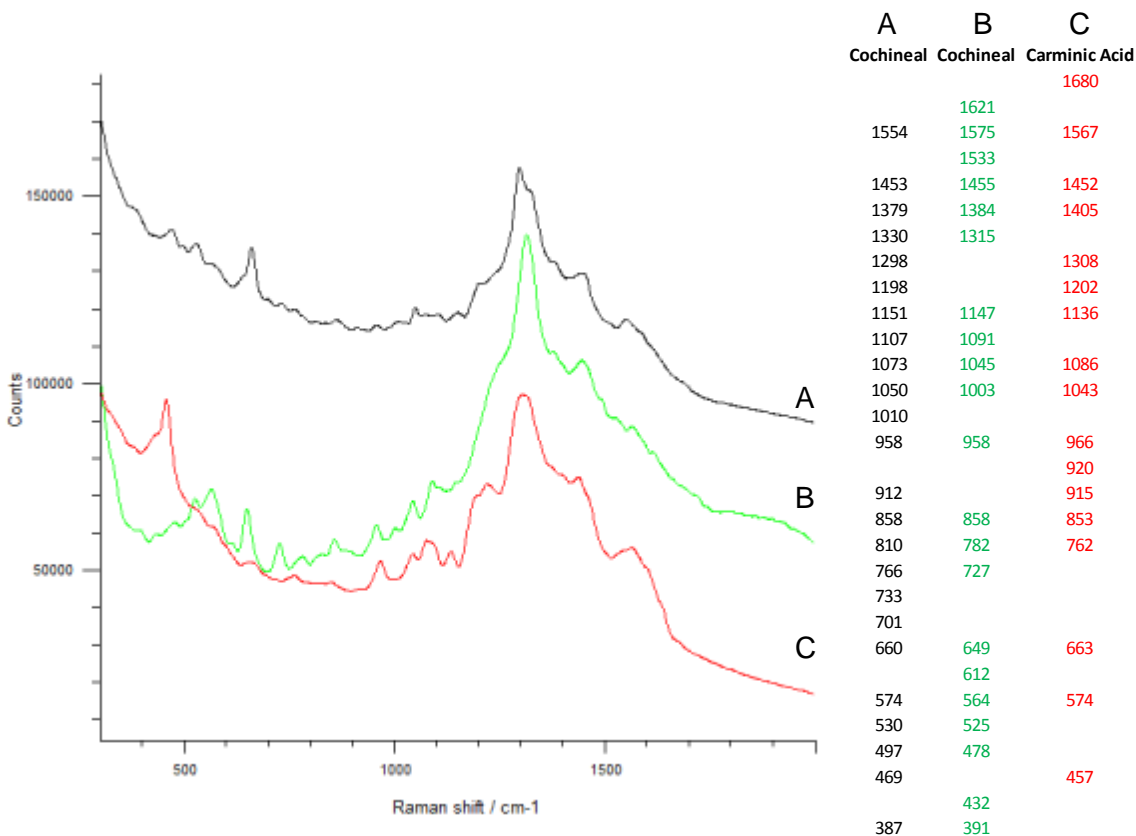


Figure 19. Raman spectra of 25% formic acid extraction from mordanted cochineal reference fibers acquired both off the fiber (A) and on the fiber (B) compared to 0.001 M carminic acid (C). All spectra obtained at UCLA using 785nm laser at 0.25% for 10 sec.

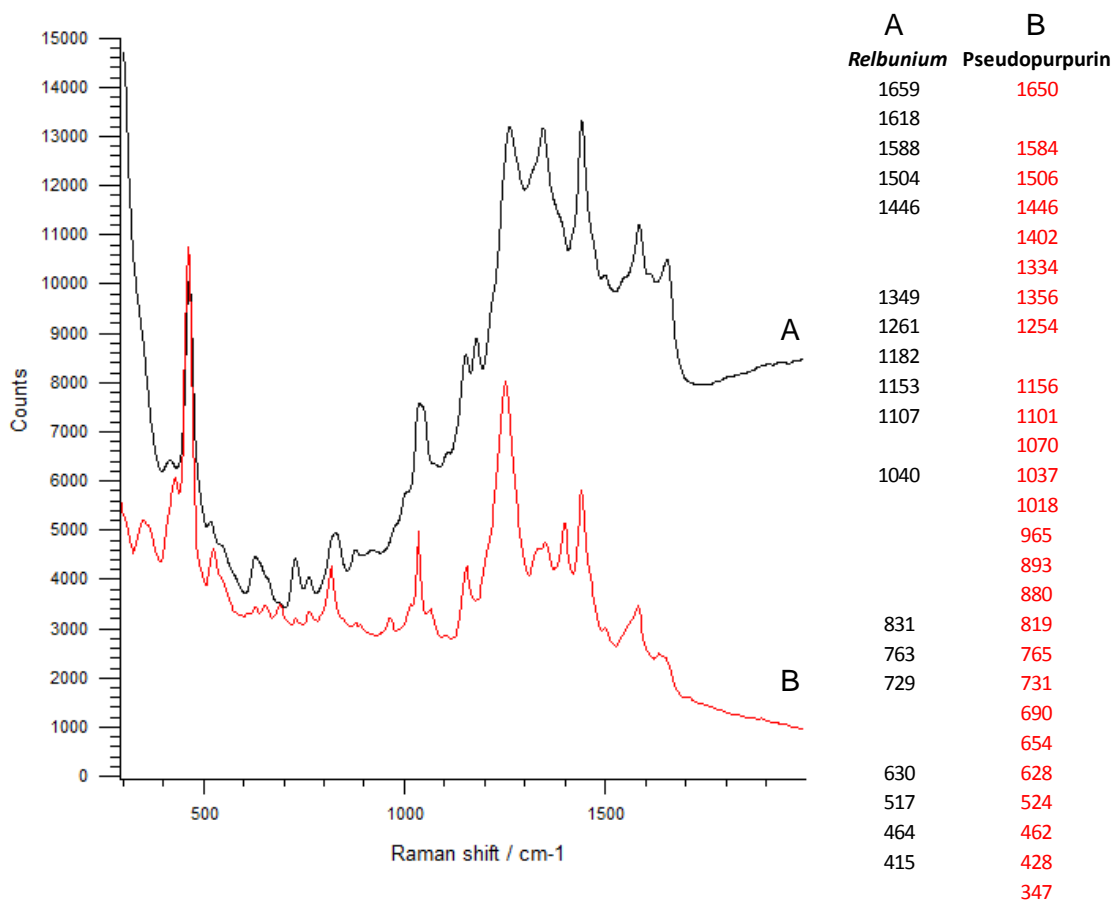


Figure 20. Raman spectra of 25% formic acid on-the-fiber extraction from mordanted *R. ciliatum* (A) compared to pseudopurpurin chemical standard (B). A at UCLA using 785 nm laser at 0.25% for 10 sec with 2 accumulations. B acquired at LACMA using 785nm laser at 1% for 5 sec.

6.3.4. Liquid micro-extraction with HCl in MeOH and H₂O

Overall, dyes prepared with liquid extraction using HCl in MeOH and H₂O provided more consistent and reproducible results than those extracted using formic acid. When HCl in MeOH and H₂O in a 2:1:1 ratio by volume was added to the carminic acid standard, the results were consistent with carminic acid at a low pH (Figure 21). When the HCl solution and carminic acid was heated for 10 minutes as required for extraction of the dye from the fiber, the strongest peak normally occurring around 1300 cm⁻¹ was shifted to 1316 cm⁻¹, which is consistent with cochineal at a very low pH [95]. However when the HCl extraction solution was applied to reference fibers of mordanted cochineal and heated for 10 minutes, the results were more

similar to carminic acid combined with HCl solution without heating. Results for cochineal acquired with 633 nm laser were more pronounced and consistent than data acquired using 785 nm laser (Figure 21). The 633 nm laser has a wavelength closer to the maximum absorbance of the AgNPs, which provides an enhancement to the SERS signal.

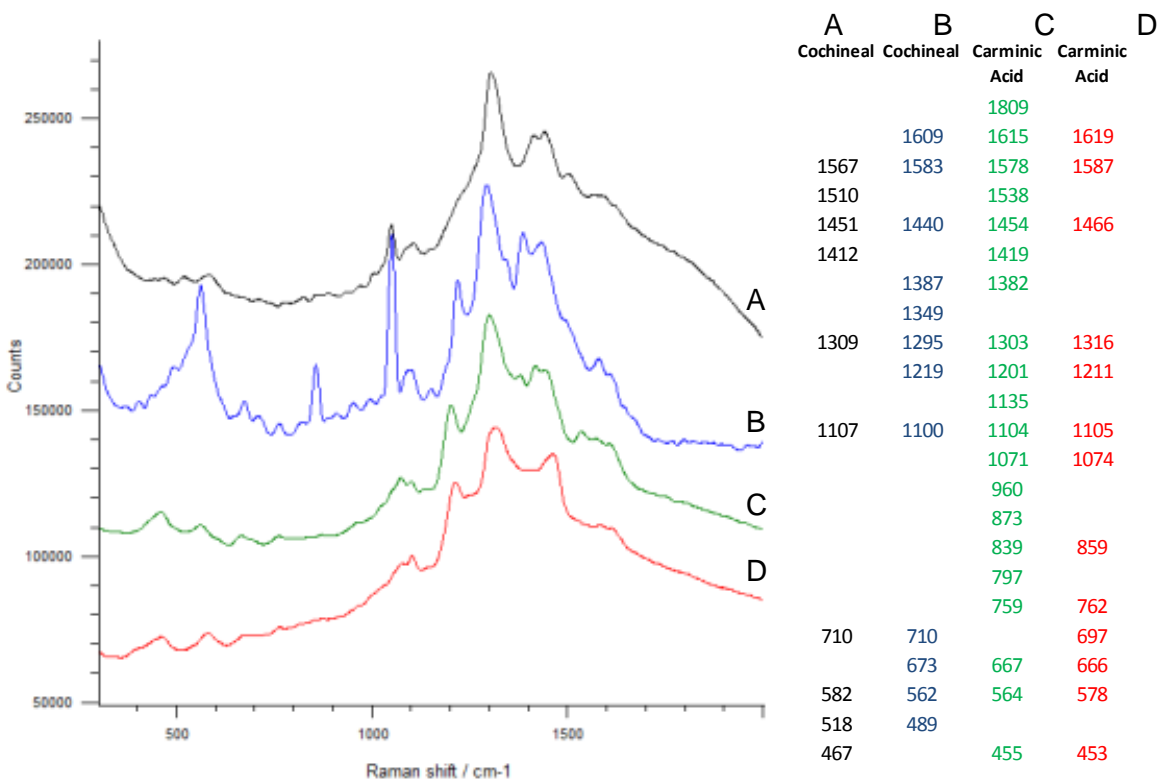


Figure 21. Raman spectra of liquid extraction using HCl in MeOH and H₂O on mordanted cochineal reference fibers (A and B) compared to 0.001M carminic acid combined with HCl in MeOH and H₂O both unheated (C) and heated for 10 minutes (D). The large peak at 1050 cm⁻¹ in the spectrum B is due to the KNO₃ added to the AgNPs. Spectra acquired at UCLA with the following parameters: A: 785nm laser at 0.25% for 10 seconds; B: 633nm laser at 0.25% for 10 seconds, C: 633nm laser at 0.01% for 10 seconds; D: 633nm at 0.25% for 10 seconds with 2 accumulations.

When the solution of HCl in MeOH and H₂O in a 2:1:1 ratio by volume was added to the purpurin chemical standard without heating the extraction solution, the results matched the purpurin standard with the exception of a peak at 1293 cm⁻¹ (Figure 22). However when the

solution was heated for 10 minutes as required during an extraction process from fiber samples, the results matched the spectrum of alizarin including a prominent peak around 1444 cm^{-1} (Figure 22), which is consistent with analysis of alizarin at a very low pH [68]¹⁵.

When the micro HCl liquid extraction was applied to *Relbunium* dyed reference fibers, the results were inconsistent and provided poor match for any chemical standard (Figure 23Figure 23). HCl is a very strong acid and capable of decomposing the fiber substrate, generating a series of other species in solution that may interfere with SERS analysis of the dye. More research is required to identify the chemical composition resulting from this extraction method, as there may be a combination of different anthraquinones and/or degradation products contributing to the spectra. A higher pH may be more appropriate for the extraction of this dye using a micro liquid extraction.

¹⁵ It is not clear why the SERS spectrum for purpurin is indistinguishable from alizarin at very low pH. The adsorption of the molecule to on the surface of the AgNPs at a very low pH may favor an orientation that does not provide significant enhancement of the hydroxyl group that distinguishes purpurin from alizarin. However, purpurin may lose a hydroxyl group at this pH degrading to alizarin. Analysis using another method such as HPLC or MS is required to determine if this is the case.

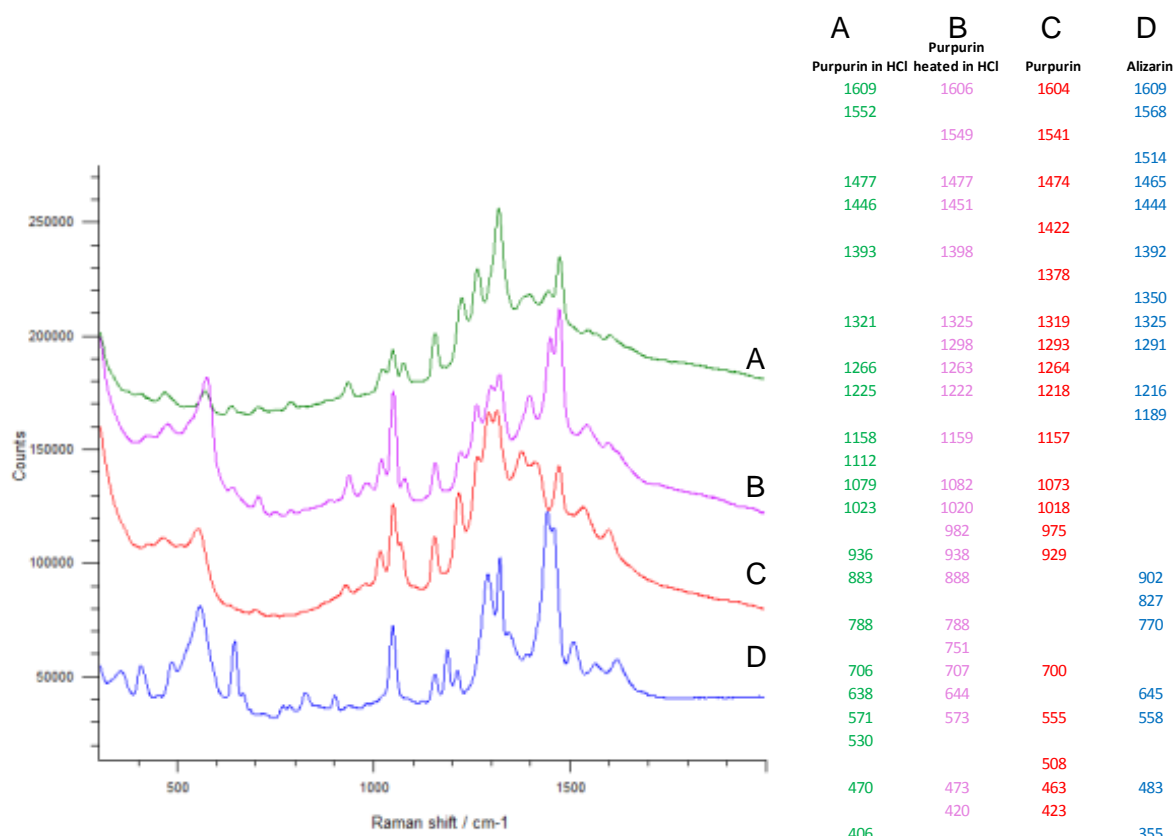


Figure 22. Raman spectra of 0.001M purpurin combined with HCl in MeOH and H₂O both unheated (A) and heated for ten minutes (B) compared to 0.001M solutions of purpurin (C) and alizarin (D). Spectra acquired at UCLA with the following parameters: A: 633nm laser at 0.01% for 10 seconds with 2 accumulations; B: 633nm laser at 0.25% for 10 seconds; C: 633nm laser at 0.25% for 10 seconds with 2 accumulations; D: 785nm laser at 0.25% for 10 seconds with 2 accumulations.

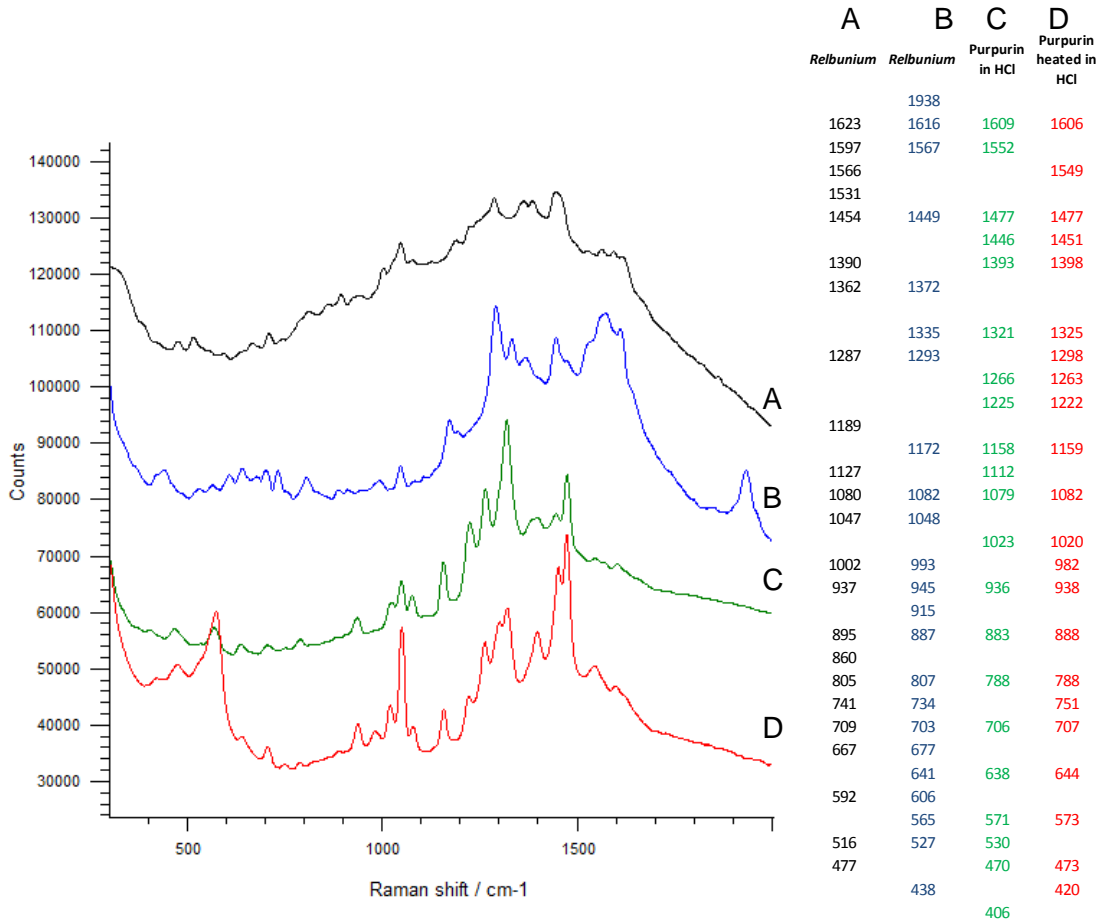


Figure 23. Raman spectra of liquid extraction using HCl in MeOH and H₂O on mordanted *Relbunium ciliatum* reference fibers (A and B) compared to 0.001M solutions of purpurin combined with HCl in MeOH and H₂O both unheated (C) and heated (D). *Relbunium* provided very inconsistent spectra and unclear match to any chemical standard. Spectra acquired at UCLA with the following parameters (listed by spectrum color): Black: 785nm laser at 0.25% for 10 seconds; Blue: 633nm laser at 0.25% for 10 seconds; Green: 633nm laser at 0.1% for 10 seconds with 2 accumulations; Red: 633nm laser at 0.25% for 10 seconds.

6.3.5. Summary of findings from SERS methods

Carminic acid was detected from cochineal using each analytical method tested. By comparison, *Relbunium* was more difficult to analyze with every technique used. The HCl liquid proved to be too strong for the analysis of *Relbunium*. Results using this technique were inconsistent and difficult to acquire, and it could not distinguish between purpurin and alizarin due to the low pH of the extraction. Though this technique can determine the difference

between plant based red dyes and cochineal, it cannot distinguish between different anthraquinone molecules found in plant dyes.

When pre-treated with either HF or formic acid, *Relbunium* provided a good match for pseudopurpurin, which is the primary compound of the dye. However using on-the-fiber analysis without extraction, the results were consistent with purpurin rather than pseudopurpurin. This could be for a multitude of reasons: 1) both molecules are present in the dye and this method may provide conditions more conducive to analysis of purpurin; 2) at this pH the chemical mechanism for adsorption on pseudopurpurin on the surface of the AgNPs may not provide strong enhancement of the carboxylic functional group that distinguishes pseudopurpurin and purpurin; or 3) the pH of the extraction may cause pseudopurpurin to lose its carboxylic group, forming purpurin.

Samples prepared with HCl solution were more consistent within a given sample than for other techniques where data was acquired on-the-fiber. Because the dye is extracted and deposited as a liquid on a glass slide, the sample distribution and AgNPs distribution was far more homogenous. However, the low pH of the extraction solution is known to alter the dye molecules, making their identification difficult and less reliable. All on-the-fiber application methods (extractionless, HF vapor, and formic acid) required multiple attempts and often a prepared sample would not provide results. This was due in large part to the heterogeneous distribution and thickness of AgNPs applied to the surface of the fiber sample. HF micro-chamber provided the cleanest match between yarns prepared using a dyestuff and their corresponding chemical standards. It also provided the most reproducible reliable method for on-the-fiber analysis.

In addition to the success of the extraction, the quality of the data is dependent on properties of the AgNPs. Further research may help to improve the AgNP synthesis and aggregation. Also,

during the final six weeks of this study, the 633nm laser was made available on the Raman spectrometer at UCLA. Compared to the 785nm laser, the data was cleaner and the analyte peaks more pronounced because this laser is closer to the resonance of the AgNPs.

6.4 Dye characterization of archaeological samples using SERS and FORS

6.4.1. Extractionless on-the-fiber SERS

Archaeological samples were first analyzed using extractionless on-the-fiber SERS though the only sample to provide a spectrum was T-130A (

Figure 24). The most prominent peaks for T-130A are shifted in comparison to both purpurin and carminic acid in neutral conditions. The T-130A peaks around 1363 1334 cm^{-1} are similar to purpurin (1357 and 1325 cm^{-1}) suggesting that the sample may include a plant based red dye such as *Relbunium*.

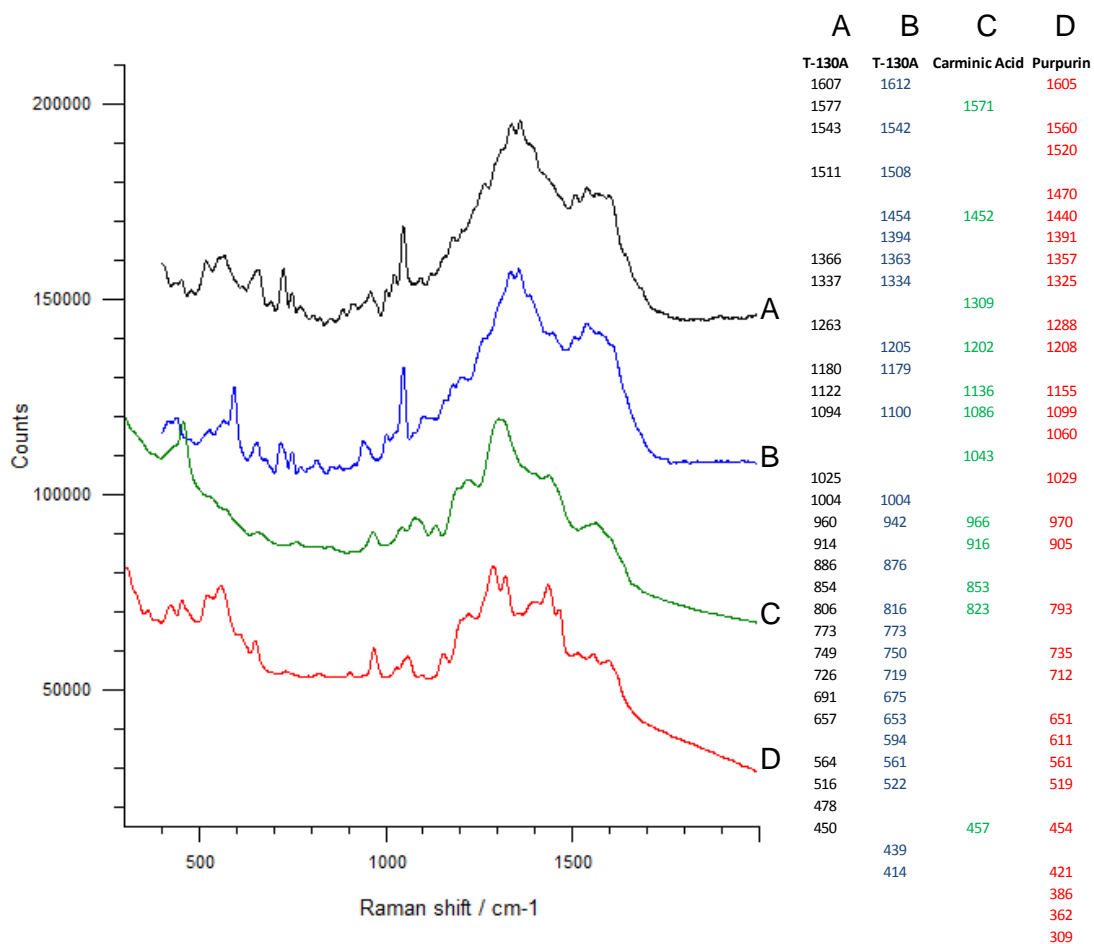


Figure 24. Raman spectra of sample T-130A based on extractionless on-the-fiber SERS without extraction (A and B) compared to carminic acid (C) and purpurin (D) both at neutral pH. The peaks at 1050 cm^{-1} in spectra A & B are due to the KNO_3 in the AgNPs. All data acquired using 785 nm laser.

6.4.2. On-the-fiber SERS with formic acid micro-extraction

Archaeological samples were further analyzed using 25% formic acid in ethanol and spectra were obtained from two additional samples: T-69 (Figure 25) and 119.000.029 (Figure 26). The signal for T-69 was weak and the presence of KNO_3 from the AgNPs at 1050 cm^{-1} was prominent suggesting that the dye molecules were not adequately extracted. Furthermore the resulting spectrum was not reproducible. It however contained some of the characteristic peaks for pseudopurpurin (at 1254 cm^{-1} and 1506 cm^{-1}) and for *Relbunium* reference sample extracted with formic acid (Figure 25). Other characteristic peaks at 462 cm^{-1} and peaks above 1550 cm^{-1} were not present in the spectrum of sample T-69.

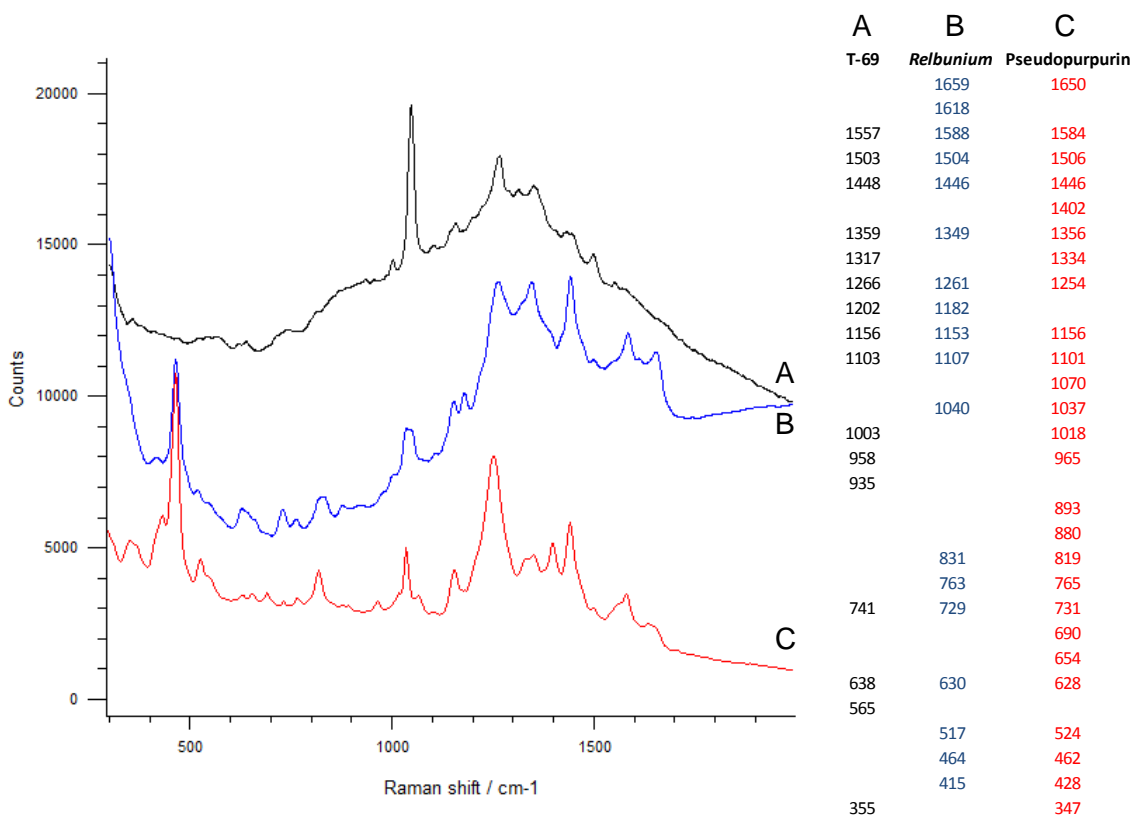


Figure 25. Raman spectra of sample T-69 analyzed using 25% formic acid (A) compared to *Relbunium ciliatum* analyzed with the same method (B) and pseudopurpurin standard (C). Neither spectrum was reproducible, though both (A and B) share common peaks with pseudopurpurin. The large peak at 1050 cm^{-1} in spectrum A is due to the KNO_3 added to the AgNPs. Spectra A and B were acquired at UCLA using 785 nm

laser at 0.25% for 10 sec, B with 2 accumulations. Spectrum C was acquired at LACMA using 785nm laser at 1% for 5 sec.

The Raman signal obtained from sample 119.000.029 was stronger than that from sample T-69, though the results were not reproducible (Figure 26). While the spectrum of sample 119.000.029 contains some corresponding peaks to pseudopurpurin and *Relbunium* extracted with formic acid, the most prominent peaks of the spectrum do not correspond to any chemical standards and/or reference material in this study. This spectrum, however, finds close parallels to previously published Raman spectra of carminic acid at low pH acquired using 1064 nm laser and AgNPs prepared with hydroxylamine [95]. Additionally, a different spectrum from this sample was acquired using the same formic acid extraction method that provides a better match for carminic acid neutral pH (Figure 27). These results suggest that sample 119.000.029 was dyed with cochineal.

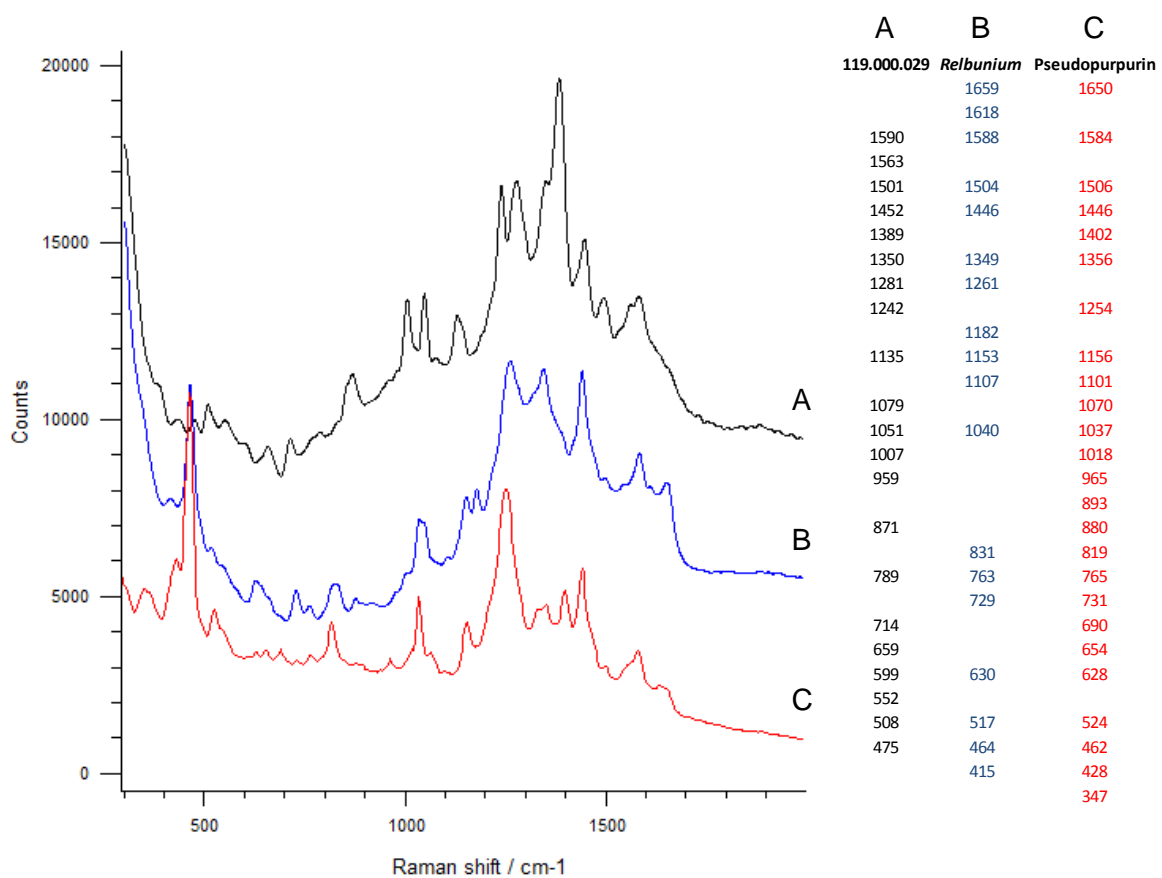


Figure 26. Raman spectra of sample 119.000.029 prepared with 25% formic acid (A) compared to *Relbunium* with the same preparation (B) and pseudopurpurin chemical standard (C). Spectra A and B were acquired at UCLA using 785 nm laser at 0.25% for 10 sec with 2 accumulations. Spectrum C acquired at LACMA using 785nm laser at 1% for 5 sec.

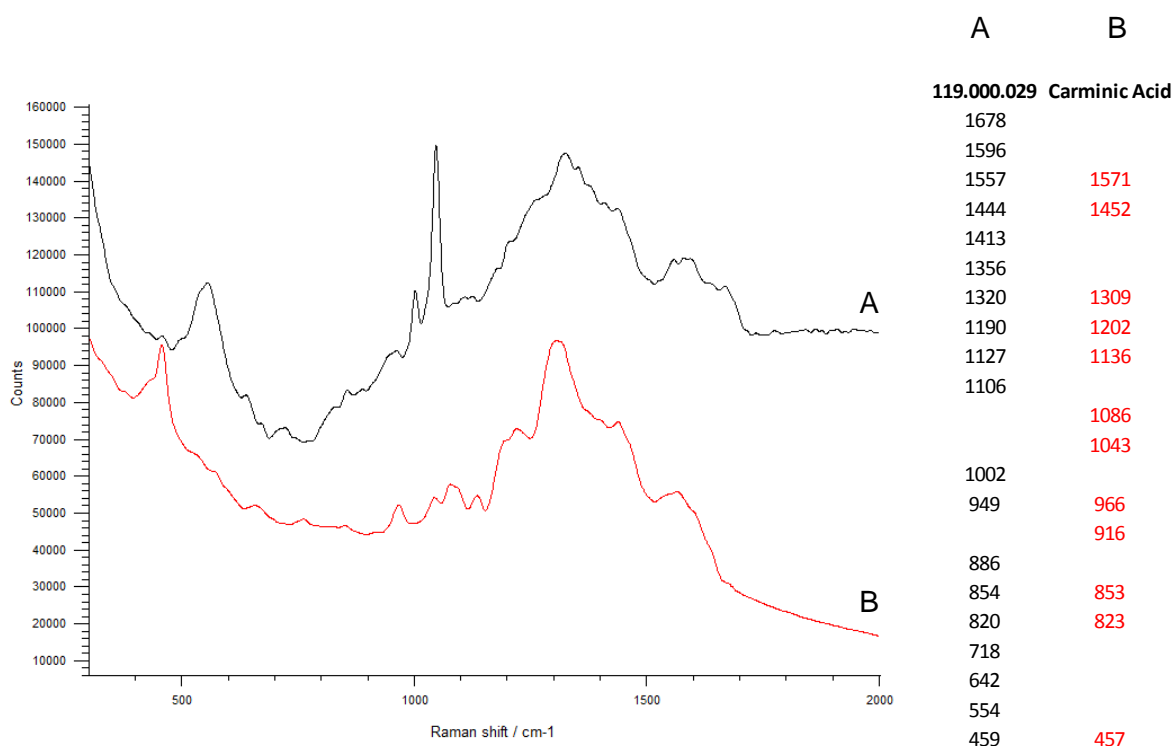


Figure 27. Raman spectra of sample 119.000.029 prepared with 25% formic acid (A) compared to carminic acid at neutral pH (B). Spectra acquired at UCLA using 785nm laser at 0.25% for 10 seconds, A with two accumulations. The large peak at 1050 cm⁻¹ in spectrum A is due to the KNO₃ added to the AgNPs.

6.4.3. Liquid micro-extraction with HCl in MeOH and H₂O

Using liquid extraction based on HCl in MeOH and H₂O results were obtained from five samples: VM04, 61.02.01, T-69, 77.10.02, and 119.000.029, with greater reproducibility for samples 77.10.02 and 119.000.029 (Figure 28) compared to VM04 and 61.02.01 (Figure 29).

Using this extraction method, spectra were also obtained from samples VM01 and T-130A however these were not comparable to known dye spectra in the database. Looking at these five samples the peak intensities did not correlate well with those of carminic acid though the peak locations matched with the exception of peak 1466 cm⁻¹, which seems shifted in the archaeological samples. Also, the peak around 1211 cm⁻¹ is reduced or absent in the archaeological samples. Given the inconsistencies when compared to spectra of carminic acid, these Raman spectra of the archaeological spectra are inconclusive as to whether cochineal

was the dyestuff used, though weathering due to burial conditions or alteration of the spectra due to the extraction method cannot be excluded.

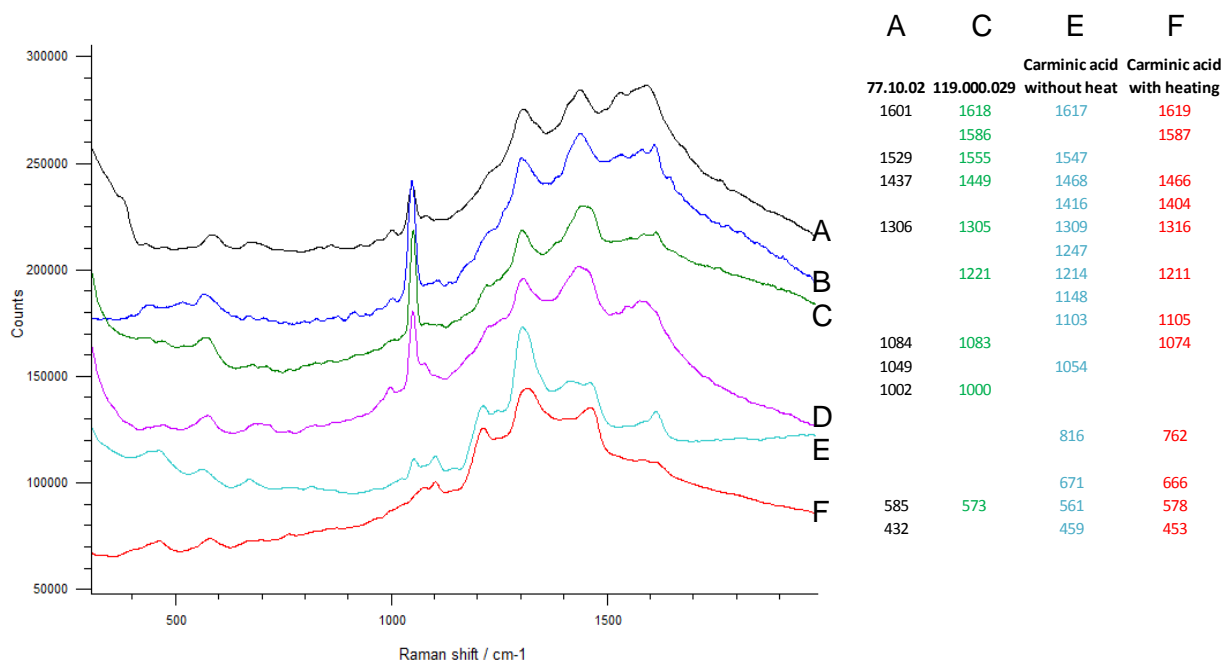


Figure 28. Raman spectra of archaeological sample 77.10.02 (A and B) and sample 119.000.029 (C and D) extracted with heated HCl compared to carminic acid prepared with HCl without heating (E) and with heating (F). All spectra acquired at UCLA using 633nm laser at 0.25% for 10 seconds and 2 accumulations with the following exceptions: D acquired at 0.01% strength; A and B acquired with 1 accumulation. The large peaks at 1050 cm^{-1} are due to KNO_3 in the AgNPs.

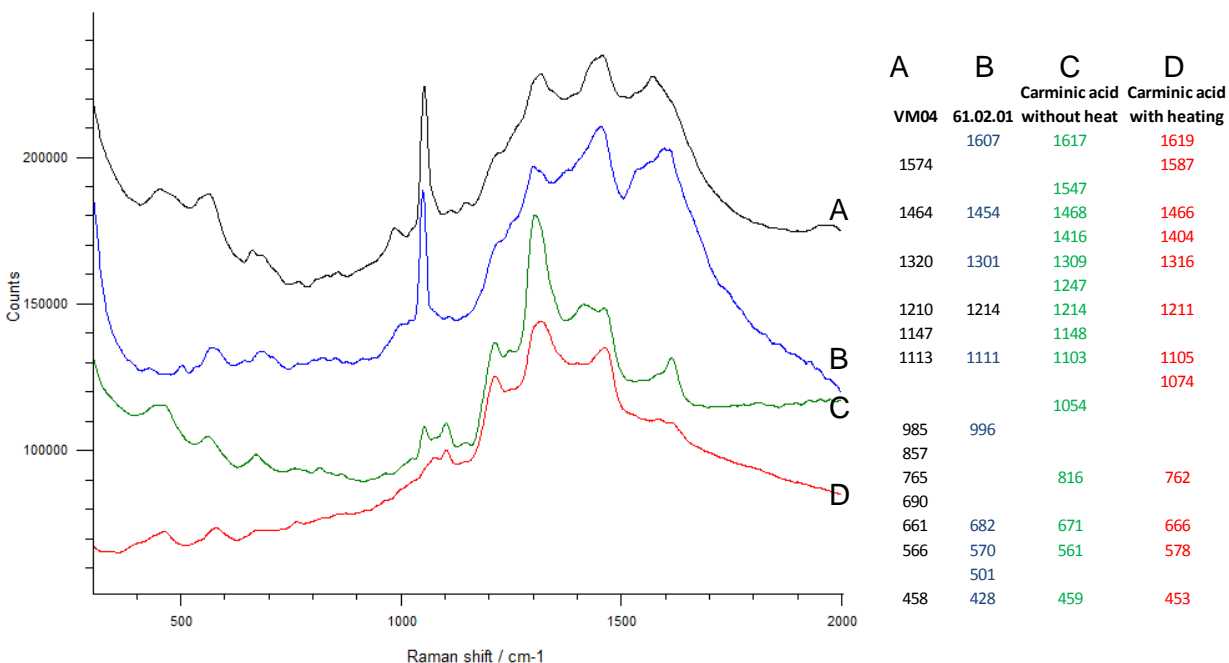


Figure 29. Archaeological samples VM04 (A) and 61.02.01 (B) extracted with heated HCl compared to carminic acid prepared with HCl without heating (C) and with heating (D). All samples acquired at UCLA using 633nm laser at 0.25% for 10 seconds with 2 accumulations. The large peaks at 1050 cm^{-1} are due to KNO_3 in the AgNPs.

6.4.4. FORS analysis of archaeological samples

FORS provided another analytical tool for the identification of the dyestuff in the samples (figure 30). Reflectance spectra of the archaeological samples showed two absorption maxima (λ_{max} Abs) in the visible between 525–535 nm and λ_{ab} 555–570 nm which are characteristic of cochineal red [97, 98]. The reflectance maximum (λ_{max} R) between 415–435 nm also typical of cochineal was not evident in these samples. However when cochineal is complexed with metal ions from the mordanting process, this band is known to shift considerably depending on the metal type [97]. Cochineal is clearly distinguished from madder species which have absorption maximum (λ_{max} Abs) between 505–515 nm and 540–550 nm [97]. This data suggests that these archaeological samples contained cochineal dye.

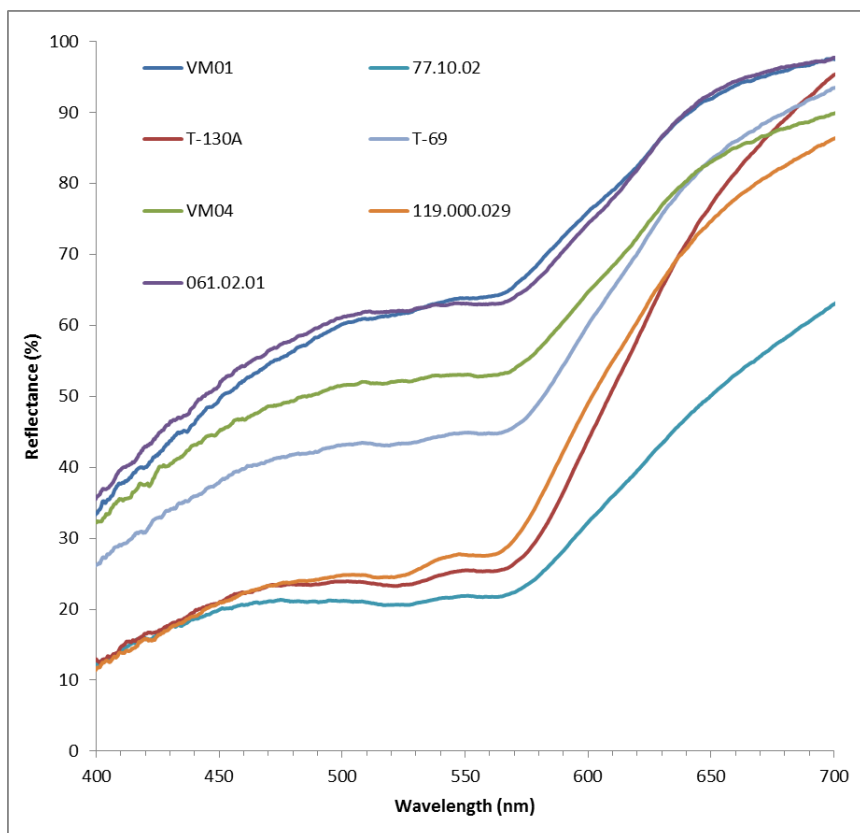


Figure 30. FORS reflectance data of archaeological samples indicating absorption maxima characteristic of cochineal red.

6.4.5. Summary of findings

Archaeological samples were analyzed with SERS using three different extraction approaches: on-the-fiber extractionless, on-the-fiber micro-extraction with formic acid, and HCL/MeOH heated liquid extraction; HF micro extraction was eliminated from this study before archaeological samples were investigated. Liquid extraction using HCl provided the best data of all the sample preparation methods tested. Data from different preparation techniques using SERS were acquired from sample 119.000.029. Samples 77.10.02, 119.000.029, and VM04 provided potential matches for carminic acid, suggesting they may contain cochineal. Data from sample T-130A contained similar peaks to purpurin and sample T-69 to pseudopurpurin, suggesting they may contain *Relbunium*, however for the match for both is poor and results remain inconclusive. Samples 77.10.02 and T-69 are finely woven Malena style textiles, while

119.000.029 is a finely woven Wari textile. Further analysis is required to draw conclusions.

Spectra comparable to known dye spectra were not acquired from samples VM01 or 061.02.01.

FORS spectra pointed to the consistent use of cochineal, though mixtures with *Relbunium* (as indicated in sample T-130A and suggested in sample T-69) cannot be excluded.

The difficulty in analyzing archaeological dyes using SERS has a number of plausible reasons.

First, the dye molecules could be degraded. While the resilient bright colors of the samples suggest that dye molecules are present, the dye may contain degradation products contributing to low signal to noise ratio. Second, because there may be more than one organic dye present in the archaeological samples, the spectra may contain peaks from multiple dyes. Third, there are undoubtedly archaeological contaminants present on the fibers. Because SERS is highly sensitive analytical technique, contamination can cause analytical uncertainties.

Chapter 7 Conclusions

7.1 SERS performance

Identification of dye molecules used in coloring archaeological textiles is a challenge regardless of the technique employed. Based on the results of this study, SERS provides a number of advantages as well as a number of challenges. SERS offered clear distinction between cochineal and *Relbunium* reference samples, demonstrating that regardless of the extraction method used, SERS can clearly distinguish these two dyes. Furthermore data are available within seconds and the experiment requires a fraction of a fiber, making this technique far more approachable where sampling limitations are of a concern.

SERS was challenging in the interpretation of results, which can be complicated by the variability in the spectra affected by the chemical environment (pH). The proper identification of a spectrum requires an understanding of how the SERS spectrum of each dye changes according to the pH. Some anthraquinones such as carminic acid are more readily identified at a low pH, while anthraquinones present in *Relbunium* are more difficult to analyze when extracted with a strong acid.

With all extraction techniques, there was large variability between the different points of acquisition both within an individual fiber and among fibers from the same sample. This provided a challenge in distinguishing between spectra of the dye molecule from that of AgNPs and contaminants. Removing possible surface contaminants perhaps using a sonication method and having greater control of the distribution of the AgNPs on the surface of the sample could potentially result in more reproducible spectra. However the pH appeared to be problematic for analysis of pH sensitive samples using this technique.

There are a number of avenues to further this study of SERS methodologies for archaeological dye analysis regarding these challenges. The benefit of the liquid extraction using HCl was the

homogeneity of the sample and the distribution of AgNPs on the glass surface, though the pH appears to be too low for analysis of *Relbunium*. Liquid extraction by other means such as a chelating agent such as EDTA may be beneficial. Also, rinsing citrate from the AgNPs and re-concentrating the colloid may improve interaction between AgNPs and the sample molecule, thereby improving reproducibility.

Based on SERS spectra in combination with FORS data, it appears that the archaeological samples all contain cochineal, regardless of their motif type. One sample, T-130A provided a match for a plant-based dye and T-69 partial identification. Further analysis would be required to make clear conclusions on the dyes present in the archaeological samples and to assess whether mixtures were used.

7.2 Future research

Based on the results from this study there are a number of areas for improvement and further investigation that could be recommended. For further investigation into the archaeological samples the following suggestions are made:

1. Further investigation into the removal of burial contaminants of the archaeological material.
2. Results of archaeological material using SERS would benefit from validation using another analytical technique due to the ambiguity of results achieved.
3. Based on the high reproducibility of spectra on reference material using HF, this extraction technique is most likely to provide results for archaeological material.
4. Include brown, purple, and yellow archaeological samples because they are like to include red dyes either in combination with other dyes, or they could represent faded red dyes.

References

1. Saltzman, M. *Analysis of dyes in museum textiles or, you can't tell a dye by its color*. in *Textile Conservation Symposium in Honor of Pat Reeves, 1 February 1986*. 1986. The Conservation Center.
2. Antunez de Mayolo, K.K., *Peruvian Natural Dye Plants*. Economic botany, 1989. **43**(2): p. 181-191.
3. Wallert, A. and R. Boytner, *Dyes from the Tumilaca and Chiribaya Cultures, South Coast of Peru*. Journal of Archaeological Science, 1996. **23**(6): p. 853-861.
4. Saltzman, M.A.X., *The Identification of Dyes in Archaeological and Ethnographic Textiles*, in *Archaeological Chemistry?II*. 1978, AMERICAN CHEMICAL SOCIETY. p. 172-185.
5. Hofenk de Graaff, J.H., *The Colorful Past: Origins, Chemistry and Identification of Natural Dyestuffs*. 2004, London: Archetype Publications Ltd.
6. Agnes Timar-Balazsy, D.E., *Chemical Principles of Textile Conservation*. Butterworth-Heinemann Series in Conservation and Museology, ed. A. Oddy. 1998, Oxford, UK: Elsevier Butterworth-Heinemann.
7. Cardon, D., *Natural Dyes: Sources, Tradition, Technology and Science*. 2007, London: Archetype Publications Ltd.
8. Roquero, A., *Tintes y tintoreros de América: catálogo de materias primas y registro etnográfico de México, Centro América, Andes Centrales y Selva Amazónica*. 2006: Ministerio de Cultura.
9. Patel, K., et al., *Identification of dyestuffs used in Peruvian ancient textiles*, in *Dyes in History and Archaeology 34*. 2015: University Ecclesiastical Academy of Thessaloniki, Greece.
10. Higgitt, C., C. McEwan, and T. Deviese. *The British Museum. Andean textiles organic colourants, biological sources and dyeing technologies*. http://www.britishmuseum.org/research/research_projects/all_current_projects/andean_textiles/in_the_lab.aspx. [cited 2016 04/2016].
11. Schweppe, H., *Identification of dyes in historic textile materials*, in *Historic textile and paper materials: Conservation and characterization*. 1986, American Chemical Society. p. 153-174.
12. Schweppe, H., *Handbuch der Naturfarbstoffe. Vorkommen. Verwendung. Nachweis*. 1993: Ecomed Verlagsgesellschaft.
13. Boucherie, N., *La couleur dans la civilisation Nasca : production tinctoriale et picturale*. 2014.
14. Rambaldi, D.C., et al., *Surface-enhanced Raman spectroscopy of various madder species on wool fibers: the role of pseudopurpurin in the interpretation of the spectra*. Journal of Raman Spectroscopy, 2015.

15. Phipps, E., *Woven to shape: a pre-Columbian trapezoidal tunic from the South Central Andes in the Metropolitan Museum of Art*. Textile Society of America Symposium Proceedings, 2008.
16. Wouters, J. and N. Rosario-Chirinos, *Dye analysis of pre-Columbian Peruvian textiles with high-performance liquid chromatography and diode-array detection*. Journal of the American Institute for Conservation, 1992. **31**(2): p. 237-255.
17. Rodriguez, L.C. and M.A. Mendez, *Direction of dispersion of cochineal (Dactylopius coccus Costa) within the Americas*. Antiquity, 2001. **75**(287): p. 73-77.
18. Brunello, F., *The art of dyeing in the history of mankind*. 1973: Aatcc.
19. Phipps, E., *Cochineal red: the art history of a color*. 2010: Metropolitan Museum of Art.
20. Donkin, R.A., *Spanish red: an ethnogeographical study of cochineal and the Opuntia cactus*. Transactions of the American Philosophical Society, 1977: p. 1-84.
21. Roquero, A., *Identification of red dyes in textiles from the Andean region*. Textile Society of America Symposium Proceedings, 2008(Paper 230).
22. Bremer, B. and J.F. Manen, *Phylogeny and classification of the subfamily Rubioideae (Rubiaceae)*. Plant Systematics and Evolution, 2000. **225**(1-4): p. 43-72.
23. Boytner, R., *Class, Control, Power: The Anthropology of Textile Dyes at Pacatnamu*, in *Andean Textile Traditions: Paper from the 2001 Mayer Center Symposium at the Denver Art Museum*, M. Young-Sánchez and F.W. Simpson, Editors. 2006, Denver Art Museum: Denver, CO. p. 43-74.
24. Mouri, C. and R. Laursen, *Identification of anthraquinone markers for distinguishing Rubia species in madder-dyed textiles by HPLC*. Microchimica Acta, 2012. **179**(1-2): p. 105-113.
25. Vincent Daniels, T.D., Marei Hacke and Catherine Higgitt, *Technological insights into madder pigment production in antiquity* The British Museum Technical Research Bulletin, 2014. **8**: p. 13-28.
26. Hill, R. and D. Richter, *Anthraquinone Pigments in Galium*. Proceedings of the Royal Society of London. Series B, Biological Sciences, 1937. **121**(825): p. 547-560.
27. de Mayolo, K.K.A., *Peruvian natural dye plants*. Economic botany, 1989. **43**(2): p. 181-191.
28. Jolie, E.A., et al., *Cordage, Textiles, and the Late Pleistocene Peopling of the Andes*. Current Anthropology, 2011. **52**(2): p. 285-296.
29. Mengoni Goñalons, G.L., *Camelids in ancient Andean societies: A review of the zooarchaeological evidence*. Quaternary International, 2008. **185**(1): p. 59-68.
30. Saltzman, M., *Identifying Dyes in Textiles*. American Scientist, 1992. **80**(5): p. 474-481.
31. Saltzman, M. and A.M. Keay, *The Identification of Colorants in Ancient Textiles*. Dyestuffs, 1963. **44**(8): p. 241-51.

32. Zhang, X., et al., *Identification of Yellow Dye Types in Pre-Columbian Andean Textiles*. Analytical Chemistry, 2007. **79**(4): p. 1575-1582.
33. Barnard, H. and R. Boytner, *Textile dyes in pre-Columbian northern Chile*, in *Dyes in History and Archaeology 34*. 2015: University Ecclesiastical Academy of Thessalniki, Greece. p. 19.
34. Boytner, R., *Textiles from the Lower Osmore Valley, Southern Peru: A Cultural Interpretation*. Andean Past, Latin American Sutides Program, Cornell Univeristy, 1998. **5**: p. 335-356.
35. Salazar, D., et al., *Interaction, social identity, agency and change during Middle Horizon San Pedro de Atacama (northern Chile): A multidimensional and interdisciplinary perspective*. Journal of Anthropological Archaeology, 2014. **35**: p. 135-152.
36. Bruno, M.C., *Practices and Processes of Agricultural Change in the Ancient Lake Titicaca Basin*. American Anthropologist, 2014. **116**(1): p. 130-145.
37. Phipps, E.S., Nobuko, *Tracing Cochineal Through the Collection of the Metropolitan Museum*. Textile Society of American Symposium Proceedings, 2010. **Paper 44**.
38. Boytner, R., *The Pacatnamu Textiles: A Study of Identity and Function*. 1998, University of California, Los Angeles: Los Angeles, CA.
39. Martoglio, P.A., et al., *Unlocking THE SECRETS OF THE PAST*. Analytical chemistry, 1990. **62**(21): p. 1123A-1128A.
40. Eitel, B., et al., *GEOARCHAEOLOGICAL EVIDENCE FROM DESERT LOESS IN THE NAZCA-PALPA REGION, SOUTHERN PERU: PALAEOENVIRONMENTAL CHANGES AND THEIR IMPACT ON PRE-COLUMBIAN CULTURES**. Archaeometry, 2005. **47**(1): p. 137-158.
41. Towle, M.S., *The Ethnobotany of Pre-Columbian Peru*. Second Printing ed. 1961, New York: Wenn-Gren Foundation for Anthropological Research Inc.
42. Ángeles Falcón, R. and D. Pozzi-Escot, *Middle Horizon textiles: evidence from Huaca Malena Asia valley*. Boletín de arqueología PUCP, 2000. **4**.
43. Falcón, R.Á. and D. Pozzi-Escot, *Del Horizonte Medio al Horizonte Tardío en la Costa Sur Central: el caso del valle de Asia*. Bull. Inst. fr. études andines, 2004. **33**(3): p. 861-886.
44. Denise Pozzi-Escot, R.Á., *Textiles de Huaca Malena*. 2011, Lima: Universidad Nacional Mayor de San Marcos, Facultad de Letras y Ciencias Humanas, Instituto del Pensamiento Peruano y Latinoamericano : Golder Associates Perú.
45. Cornell, R.M. and U. Schwertmann, *The Iron Oxides: Structure, Properties, Reactions, Occurrences and Uses*. 2nd ed. 2003, Weinheim: WILEY-VCH Verlag GmbH&Co. KGaA.
46. Craddock, P.T., *Early metal mining and production 1995*, Edinburgh; Washington, DC Edinburgh University Press; Smithsonian University Press

47. Leona, M., J. Stenger, and E. Ferloni, *Application of surface-enhanced Raman scattering techniques to the ultrasensitive identification of natural dyes in works of art*. *Journal of Raman Spectroscopy*, 2006. **37**(10): p. 981-992.
48. Wang, P., et al., *Ultra-Sensitive Graphene-Plasmonic Hybrid Platform for Label-Free Detection*. *Advanced Materials*, 2013. **25**(35): p. 4918-4924.
49. Xu, X., et al., *Near-Field Enhanced Plasmonic-Magnetic Bifunctional Nanotubes for Single Cell Bioanalysis*. *Advanced Functional Materials*, 2013.
50. Yazdi, S.H., K.L. Giles, and I.M. White, *Multiplexed detection of DNA sequences using a competitive displacement assay in a microfluidic SERRS-based device*. *Analytical chemistry*, 2013. **85**(21): p. 10605-10611.
51. Kurth, M.L. and D.K. Gramotnev, *Nanofluidic delivery of molecules: integrated plasmonic sensing with nanoholes*. *Microfluidics and Nanofluidics*, 2013: p. 1-9.
52. Oh, Y.J., et al., *Beyond the SERS: Raman enhancement of small molecules using nanofluidic channels with localized surface plasmon resonance*. *Small*, 2011. **7**(2): p. 184-188.
53. Long, D.A., *Introduction to Raman Spectroscopy*, in *Raman Spectroscopy in Archaeology and Art History*, H.G.M. Edwards and J.M. Chalmers, Editors. 2005, The Royal Society of Chemistry: Cambridge. p. 17-40.
54. Casadio, F., et al., *Identification of Organic Colorants in Fibers, Paints, and Glazes by Surface Enhanced Raman Spectroscopy*. *Accounts of Chemical Research*, 2010. **43**(6): p. 782-791.
55. King, P.J. and L.E. Stager, *Life in Biblical Israel*. 2001, Louisville, Kentucky: Westminster John Knox Press.
56. von Bogdandy, L. and H. Jürgen Engell, *The Reduction of Iron Ores: Scientific Basis and Technology*. 1971, Berlin, New York: Springer-Verlag.
57. Kaniewski, D., et al., *Late second,Äearly first millennium BC abrupt climate changes in coastal Syria and their possible significance for the history of the Eastern Mediterranean*. *Quaternary Research*, 2010. **74**(2): p. 207-215.
58. Veldhuijzen, H.A. and T. Rehren, *Slags and the city: early iron production at Tell Hammeh, Jordan and Tel Beth-Shemesh, Israel*, in *Metals and Mines Studies in Archaeometallurgy*, S. LaNiece, D. Hook, and P. Craddock, Editors. 2007, Archetype/British Museum: London. p. 189-201.
59. Lombardi, J.R. and R.L. Birke, *A Unified Approach to Surface-Enhanced Raman Spectroscopy*. *The Journal of Physical Chemistry C*, 2008. **112**(14): p. 5605-5617.
60. Schreiner, M., M. Melcher, and K. Uhler, *Scanning electron microscopy and energy dispersive analysis: applications in the field of cultural heritage*. *Analytical and Bioanalytical Chemistry*, 2007. **387**(3): p. 737-47.

61. van der Weerd, J., et al., *Identification of black pigments on prehistoric Southwest American potsherds by infrared and Raman microscopy*. Journal of Archaeological Science, 2004. **31**(10): p. 1429-1437.
62. Chen, K., et al., *Application of surface-enhanced Raman scattering (SERS) for the identification of anthraquinone dyes used in works of art*. Journal of Raman Spectroscopy, 2006. **37**(4): p. 520-527.
63. Leona, M., *Microanalysis of organic pigments and glazes in polychrome works of art by surface-enhanced resonance Raman scattering*. Proceedings of the National Academy of Sciences, 2009. **106**(35): p. 14757-14762.
64. Leona, M. and J.R. Lombardi, *Identification of berberine in ancient and historical textiles by surface-enhanced Raman scattering*. Journal of Raman Spectroscopy, 2007. **38**(7): p. 853-858.
65. Leona, M., J. Stenger, and E. Ferloni, *Application of surface-enhanced Raman scattering techniques to the ultrasensitive identification of natural dyes in works of art*. Journal of Raman Spectroscopy, 2006. **37**(10): p. 981-992.
66. Lombardi, J.R. and R.L. Birke, *A Unified View of Surface-Enhanced Raman Scattering*. Accounts of Chemical Research, 2009. **42**(6): p. 734-742.
67. Teslova, T., et al., *Raman and surface-enhanced Raman spectra of flavone and several hydroxy derivatives*. Journal of Raman Spectroscopy, 2007. **38**(7): p. 802-818.
68. Shadi, I.T., et al., *Semi-quantitative analysis of alizarin and purpurin by surface-enhanced resonance Raman spectroscopy (SERRS) using silver colloids*. Journal of Raman Spectroscopy, 2004. **35**(8-9): p. 800-807.
69. Witnall, R., I.T. Shadi, and B.Z. Chowdhry, *The Analysis of Dyes by SERRS*, in *Raman Spectroscopy in Archaeology and Art History*, H.G.M. Edwards and J.M. Chalmers, Editors. 2005, The Royal Society of Chemistry: Cambridge. p. 17-40.
70. Whitney, A.V., R.P. Van Duyne, and F. Casadio, *An innovative surface-enhanced Raman spectroscopy (SERS) method for the identification of six historical red lakes and dyestuffs*. Journal of Raman Spectroscopy, 2006. **37**(10): p. 993-1002.
71. Leona, M., *Surface-Enhanced Raman Scattering in Art and Archaeology*. 2005. **5993**.
72. Jurasekova, Z., et al., *Extractionless non-hydrolysis surface-enhanced Raman spectroscopic detection of historical mordant dyes on textile fibers†*. Journal of Raman Spectroscopy, 2010.
73. McCreery, R.L., *Raman spectroscopy for chemical analysis*. Chemical Analysis: A Series of Monographs on Analytical Chemistry and Its Applications, ed. J.D. Winefordner. Vol. 157. 2000, New York: John Wiley & Sons.
74. Lee, P.C. and D. Meisel, *Adsorption and surface-enhanced Raman of dyes on silver and gold sols*. The Journal of Physical Chemistry, 1982. **86**(17): p. 3391-3395.

75. Idone, A., et al., *Silver colloidal pastes for dye analysis of reference and historical textile fibers using direct, extractionless, non-hydrolysis surface-enhanced Raman spectroscopy*. Analyst, 2013. **138**(20): p. 5895-5903.
76. Cañamares, M.V., et al., *Comparative SERS effectiveness of silver nanoparticles prepared by different methods: A study of the enhancement factor and the interfacial properties*. Journal of Colloid and Interface Science, 2008. **326**(1): p. 103-109.
77. Canamares, M., et al., *Comparative study of the morphology, aggregation, adherence to glass, and surface-enhanced Raman scattering activity of silver nanoparticles prepared by chemical reduction of Ag⁺ using citrate and hydroxylamine*. Langmuir, 2005. **21**(18): p. 8546-8553.
78. Leona, M., et al., *Nondestructive Identification of Natural and Synthetic Organic Colorants in Works of Art by Surface Enhanced Raman Scattering*. Analytical Chemistry, 2011. **83**(11): p. 3990-3993.
79. Casadio, F., et al., *Identification of Organic Colorants in Fibers, Paints, and Glazes by Surface Enhanced Raman Spectroscopy*. Accounts of Chemical Research, 2010. **43**(6): p. 782-791.
80. Brosseau, C.L., et al., *Ad-hoc surface-enhanced Raman spectroscopy methodologies for the detection of artist dyestuffs: thin layer chromatography-surface enhanced Raman spectroscopy and in situ on the fiber analysis*. Analytical chemistry, 2009. **81**(8): p. 3056-3062.
81. Brosseau, C.L., et al., *Surface-enhanced Raman spectroscopy: a direct method to identify colorants in various artist media*. Analytical chemistry, 2009. **81**(17): p. 7443-7447.
82. Londero, P.S., J.R. Lombardi, and M. Leona, *Laser Ablation Surface-enhanced Raman Microspectroscopy*. Analytical chemistry, 2013.
83. Prikhodko, S., et al., *New Advancements in SERS Dye Detection Using Interfaced SEM and Raman Spectromicroscopy (μ RS)*. Journal of Raman Spectroscopy, 2015.
84. Prikhodko, S.V., et al., *Interfaced SEM and micro-Raman Spectroscopy for SERS Analysis of Dyes on Single Fibers*. Microscopy and Microanalysis, 2014. **20**(S3): p. 2008-2009.
85. Cañamares, M.V. and J.R. Lombardi, *Raman, SERS, and DFT of Mauve Dye: Adsorption on Ag Nanoparticles*. The Journal of Physical Chemistry C, 2015. **119**(25): p. 14297-14303.
86. Aceto, M., et al., *A diagnostic study on folium and orchil dyes with non-invasive and micro-destructive methods*. Spectrochimica Acta Part A: Molecular and Biomolecular Spectroscopy, 2015. **142**: p. 159-168.
87. Iravani, S., et al., *Synthesis of silver nanoparticles: chemical, physical and biological methods*. Research in Pharmaceutical Sciences, 2014. **9**(6): p. 385-406.
88. Lofrumento, C., et al., *SERS detection of red organic dyes in Ag-agar gel*. Journal of Raman Spectroscopy, 2013. **44**(1): p. 47-54.

89. Platania, E., et al., *Suitability of Ag-agar gel for the micro-extraction of organic dyes on different substrates: the case study of wool, silk, printed cotton and a panel painting mock-up*. Journal of Raman Spectroscopy, 2014.
90. Frame, M. and R.Á. Falcón, *A female funerary bundle from Huaca Malena. Ñawpa Pacha*, 2014. **34**(1): p. 27-59.
91. Splitstoser, J.C. *The Parenthetical Notation Method for Recording Yarn Structure*. in *Textiles and Politics: Textile Society of America 13th Biennial Symposium Proceedings*. 2012. Washington, DC: DigitalCommons@University of Nebraska- Lincoln.
92. Houck, M.M., *Identification of textile fibers*. 2009: Elsevier.
93. Bergen, W.v. and W. Krauss, *Textile fiber atlas. A collection of photomicrographs of old and new textile fibers*. Textile fiber atlas. A collection of photomicrographs of old and new textile fibers., 1942.
94. Janaway, R.C., *Degradation of Clothing and Other Dress Materials Associated with Buried Bodies of Archaeological and Forensic Interest*, in *Advances in Forensic Taphonomy: Method, Theory, and Archaeological Perspectives*, W.D. Haglund and M.H. Sorg, Editors. 2001, CRC Press. p. 379-403.
95. Canamares, M., et al., *Surface-enhanced Raman scattering study of the anthraquinone red pigment carminic acid*. Vibrational spectroscopy, 2006. **40**(2): p. 161-167.
96. Canamares, M., et al., *Surface-enhanced Raman scattering study of the adsorption of the anthraquinone pigment alizarin on Ag nanoparticles*. Journal of Raman Spectroscopy, 2004. **35**(11): p. 921-927.
97. Gulmini, M., et al., *Identification of dyestuffs in historical textiles: Strong and weak points of a non-invasive approach*. Dyes and Pigments, 2013. **98**(1): p. 136-145.
98. Aceto, M., et al., *Non-invasive investigation on a VI century purple codex from Brescia, Italy*. Spectrochimica Acta Part A: Molecular and Biomolecular Spectroscopy, 2014. **117**: p. 34-41.